Available online at www.sciencedirect.com

SCIENCE DIRECT®

Lithos 82 (2005) 289–314

LITHOS

www.elsevier.com/locate/lithos

Geochemistry and Sr, Nd, Pb isotopic composition of the Central Atlantic Magmatic Province (CAMP) in Guyana and Guinea

Katja Deckart[a,*], Hervé Bertrand[b], Jean-Paul Liégeois[c]

[a]*Departamento de Geologia, Universidad de Chile, Plaza Ercilla 803, P.O. Box 13518, Santiago, Chile*
[b]*Laboratoire des Sciences de la Terre, UMR-CNRS 5570, ENS Lyon, 46 Allée d'Italie, F-69364 Lyon Cedex 07, France*
[c]*Isotope Geology, Africa Museum, B-3080 Tervuren, Belgium*

Received 9 February 2004; accepted 4 January 2005
Available online 26 February 2005

Abstract

The Central Atlantic Magmatic Province (CAMP) is one of the largest igneous provinces on Earth, extending more than 5000 km north to south, on both sides of the Atlantic Ocean. Its emplacement occurred about 200 Ma ago, at the Triassic–Jurassic boundary, and is linked to the initial breakup of Pangaea. Two areas of the province are studied here: French Guyana/Surinam (South America) and Guinea (West Africa), in order to document the petrogenesis and geodynamical significance of high-Ti and low-Ti basaltic magmas from the CAMP.

In Guyana, doleritic and gabbroic dykes are located on the edge of the Guiana Shield, and represent limited volumes of magma. They display low SiO_2 (47–50%), high TiO_2 (2.5–3.5%) and high FeO tholeiitic trends and show variably enriched trace element patterns ($(La/Yb)_n$=1.5–5.1). Their isotopic signature and ratios of very incompatible elements (εNd_i=+5.8 to +4.2, $(^{87}Sr/^{86}Sr)_i$=0.703–0.705, $(^{207}Pb/^{204}Pb)_i$=15.46–15.64) match a depleted PREMA (prevalent mantle)-like source. Their genesis can be modeled by ca. 15% partial melting of a lherzolite source, and a subsequent limited fractional crystallization (5–10%) or a slight upper crustal assimilation–fractional crystallization (AFC, r=0.1, Proterozoic contaminant). In Guinea, in contrast, huge volumes of CAMP magmas were intruded along the Rockelides suture and the West African craton, forming the Fouta Djalon sills and the Kakoulima laccolith. The laccolith is more than 1000 m thick. These features consist of gabbros, dolerites, diorites and mafic (gabbro) and ultramafic (dunite, wherlite) cumulates. Guinean tholeiites show high SiO_2 (51–58%), low TiO_2 (0.7–1.2%) and FeO trends, with high LILE/HFSE ratios and slight negative Nb–Ta anomalies. Isotopic signatures (εNd_i=+0.4 to −5.3, $(^{87}Sr/^{86}Sr)_i$=0.705–0.710, $(^{207}Pb/^{204}Pb)_i$=15.57–15.66) indicate a more enriched source than for Guyana as well as a higher rate of magma–upper crust interaction through an AFC process (r=0.3, Birimian crust contaminant) and, probably, an additional upper crustal contamination for the most differentiated sample.

* Corresponding author. Tel.: +56 2 6784758; fax: +56 2 6963050.
E-mail addresses: kdeckart@cec.uchile.cl (K. Deckart), Herve.Bertrand@ens-lyon.fr (H. Bertrand), jean-paul.liegeois@africamuseum.be (J.-P. Liégeois).

doi:10.1016/j.lithos.2004.09.023

This geochemical study supports the prevalence in Guinea, as for other low-Ti CAMP tholeiites, of a lithospheric mantle source, previously enriched during ancient subduction events, and preferentially reactivated in late Triassic times by edge-driven convection between cratonic and mobile belt domains. A larger contribution from a depleted asthenospheric source is required to generate high-Ti tholeiites in Guyana, which may reflect the development of CAMP rifting towards the initiation of the Central Atlantic oceanic crust.

Keywords: CAMP; Jurassic tholeiites; Mantle source; Crustal contaminants; Sr, Nd, Pb isotopes

1. Introduction

The initial fragmentation of the Pangaea supercontinent was accompanied by extensive tholeiitic magmatism now represented by sills, dykes and minor lava-flows in four continents along both sides of the Central Atlantic Ocean, on the eastern margin of North America (between Nova Scotia and Florida), Western Europe (Iberian Peninsula and France), West Africa (from Morocco to the Ivory Coast) and northern South America (French Guyana, Surinam and Brazil). This igneous province has been linked to the early Mesozoic initial opening of the Central Atlantic Ocean (e.g., Dalrymple et al., 1975; Bertrand et al., 1982; Alibert, 1985; Dupuy et al., 1988; Pegram, 1990; Bertrand, 1991; Sebai et al., 1991; Deckart et al., 1997; McHone, 2000; Hames et al., 2000; Cebriá et al., 2003; DeMin et al., 2003) and since Marzoli et al. (1999), is commonly referred to as the Central Atlantic Magmatic Province (CAMP).

Most of the CAMP investigated throughout the four circum-Atlantic continents are typical tholeiitic low-Ti continental flood basalts (CFB), which differ fundamentally from mid-ocean ridge basalts (MORB) by higher concentrations of light rare earth elements (LREE), large ion lithophile elements (LILE: e.g., K, Ba, Rb) and Th (e.g., Weigand and Ragland, 1970; Bryan et al., 1977; Bertrand et al., 1982; Alibert, 1985; Dupuy et al., 1988; Bertrand, 1991; Puffer, 2001; Cebriá et al., 2003; DeMin et al., 2003).

The relative enrichment of these elements in CAMP basalts has been long debated and has been explained by different mechanisms: (1) derivation from an enriched subcontinental lithospheric mantle source, with no or limited crustal contamination during magma ascent (e.g., Bertrand et al., 1982; Alibert, 1985; Dupuy et al., 1988; Pegram, 1990; Bertrand, 1991; Heatherington and Mueller, 1999; DeMin et al., 2003); (2) derivation from an asthenospheric MORB-like source with a more important crustal contamination (Dostal and Dupuy, 1984; Dupuy and Dostal, 1984); and (3) derivation from an incipient plume head (Morgan, 1983; White and McKenzie, 1989; Hill, 1991; Wilson, 1997; Oyarzun et al., 1997; Courtillot et al., 1999; Ernst and Buchan, 2002). In respect of (3), however, only a few publications discussed the geochemical composition of the possibly involved magmas (Oliveira et al., 1990; Janney and Castillo, 2001). The first model, derivation from an enriched subcontinental lithospheric mantle source, is the most commonly accepted.

In contrast, however, high-Ti tholeiitic dykes have been documented in Liberia (Dupuy et al., 1988; Mauche et al., 1989), French Guyana (Deckart, 1996; Bertrand et al., 1999; Nomade et al., 2002a) and nearby northern Brazil (Oliveira et al., 1990; DeMin et al., 2003), forming a narrow belt compared to the large extension of CAMP. This belt cuts through the Rockelides suture and the borders of the Guyana and West African cratons in an area corresponding to the "cul-de-sac" of the forthcoming Central Atlantic Ocean (Fig. 1).

The scope of this paper is to investigate geochemical and Nd–Sr–Pb isotope compositions of CAMP intrusive bodies (laccolith, sills and dykes) from Guinea and French Guyana/Surinam. These two poorly studied areas of CAMP, presently located on West African and South American margins, were adjacent in a 200 Ma pre-drift reconstruction (Fig. 1) and are representative of low-Ti and high-Ti tholeiites, respectively. Therefore, they offer a good opportunity to constrain the genesis and the significance of these two contrasted magma groups during the initiation of

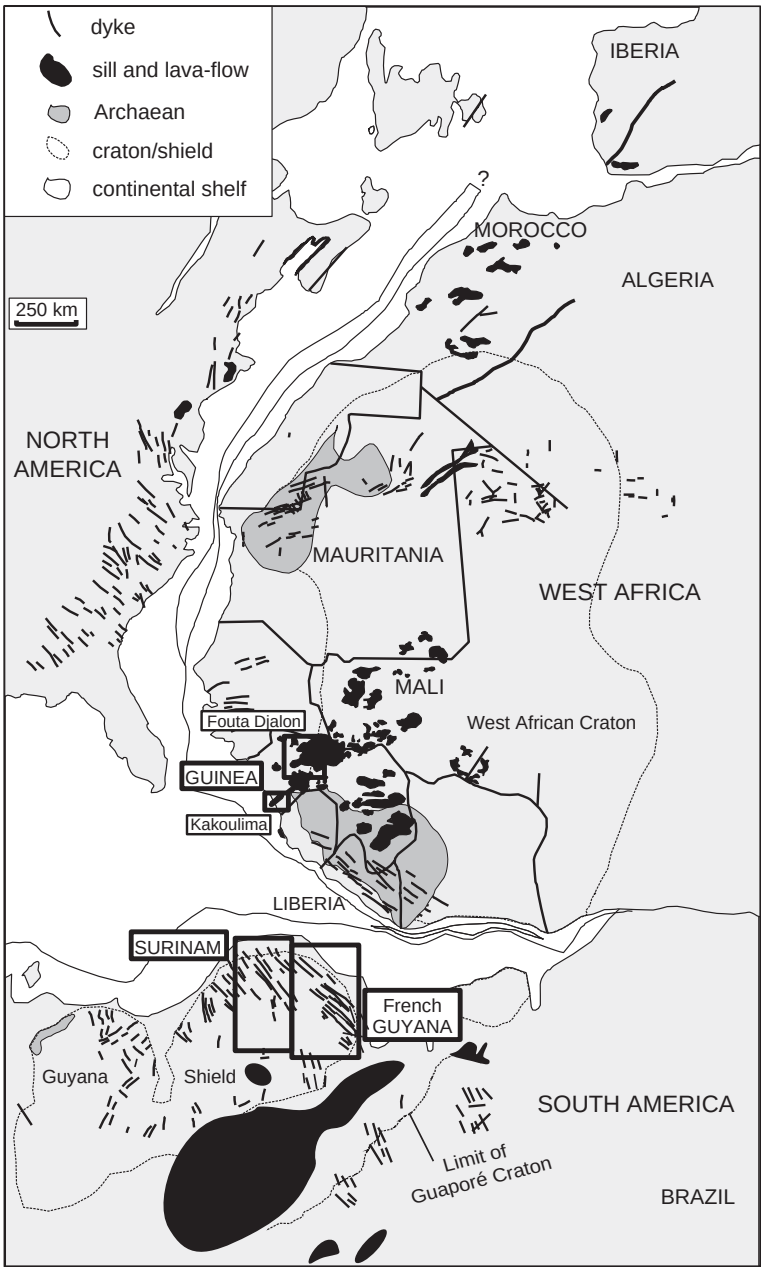

Fig. 1. Map of CAMP magmatism around the initial Central Atlantic Ocean (pre-drift reconstruction from Bullard et al., 1965; CAMP locations compiled from May, 1971; Bertrand, 1991; Deckart et al., 1997; Marzoli et al., 1999; McHone, 2000). Dykes intruding the Archaean basement in Mauritania have not yet been dated and E–W dykes in Senegal are inferred from remote survey. Boxes indicate study areas shown with more details in Figs. 2 and 3.

the breakup of Pangaea. More specifically, we address the issues of (1) the geographic grouping of the high-Ti tholeiites within CAMP and (2) whether high- and low-Ti tholeiites reflect different mantle sources, contrasting magmatic processes or crustal interaction, or the combination of these.

2. Geological setting

2.1. Basement

The basement of French Guyana and Surinam belongs to the Guyana Shield (Fig. 1), built during the Archaean and Palaeoproterozoic (Gibbs and Barron, 1983). In these two countries, it was formed essentially during the Trans-Amazonian orogeny, between 2.2 and 2.0 Ga (Bosma et al., 1983; Gruau et al., 1985; Caen-Vachette, 1988). It consists of medium- to high-grade metasediments and metavolcanics subsequently intruded by a granitoid complex, around 1.9 to 1.8 Ga (Priem et al., 1971, 1977; Bosma et al., 1983; Ledru et al., 1991). In Surinam, post-orogenic volcanoclastic sedimentation and dolerite intrusions occurred around 1.65–1.6 Ga (Priem et al., 1968, 1973; Hebeda et al., 1973), while a later low-grade metamorphic event was dated at 1.2±0.1 Ga (Hebeda et al., 1973; Bosma et al., 1983).

Most of the basement in West Africa was formed during three major orogenic events: Liberian (~2.7 Ga, Hurley et al., 1971), Eburnian (~2.1 Ga=Trans-Amazonian) affecting the Birimian terrains (Abouchami et al., 1990; Liégeois et al., 1991; Boher et al., 1992) and Pan-African (mainly 750–660 and 650–580 Ma; Liégeois et al., 1994). The Guinea CAMP province intrudes the intracratonic and boundary zone at the south-western edge of the West African craton (Archaean to Palaeoproterozoic; Fig. 1) and the adjacent Pan-African belts of Rockelides and Bassarides, which are thrust upon the craton and partly covered by the Palaeozoic Bove Basin (Villeneuve and Cornée, 1994). These old country-rocks will contrast isotopically with Jurassic mantle sources compositions.

2.2. CAMP tholeiites in Guyana and Guinea

In French Guyana/Surinam (hereafter Guyana), CAMP tholeiites occur mainly as dykes intruding the northern and eastern edges of the shield (Choubert, 1960). The general trend is NNW–SSE to N–S (Fig. 2) and differs from the dominantly NNE–SSW to NE–SW trends defined by Proterozoic dykes (Bosma et al., 1983; Choudhuri et al., 1991), although NNW-trending Proterozoic dykes may also occur (Priem et al., 1968), sometimes making the distinction difficult. To the east, the dykes form discontinuous outcrops of a few hundred metres to a few kilometres in length, probably belonging to the same dense dyke swarm extending from Cayenne-"Les Mamelles" Islands to Regina (Fig. 2a). In western French Guyana and in Surinam, the dykes become more widely spaced and can be followed along strike for several tens of kilometres. Their width is difficult to assess because of the forest cover and lateritic alteration. However, good exposures and contacts exist in the coastal region, where the dykes generally range in thickness from 0.5 m to tens of metres, but to the west of Cacao their width locally reaches 2000 m. CAMP tholeiites are also represented by horizontal sill-like structure forming the "Iles du Salut" (Devil's Islands) situated NE of Kourou. The emerged part is about 2 km in diameter and 35 m thick, but lower and upper contacts were not observed. Former studies were restricted to some dykes from Surinam and concern their petrology (Hawkes, 1966; Choudhuri, 1978a,b) or K–Ar and Rb–Sr chronology (Priem et al., 1968, 1973; Hebeda et al., 1973). More recently, a petrological study compared Jurassic and Proterozoic dykes from Guyana (Nomade et al., 2002a).

In Guinea, CAMP tholeiites were first described by Lacroix (1905). They represent huge volumes of magma intruding Archaean to Palaeozoic basement all over the country (Fig. 3). The most important outcrops are sills, formerly interpreted as lava-flows. They are particularly well developed to the northwest, forming the Fouta Djalon plateau. Individual sills may reach more than 1000 km^2 with a thickness varying from a few metres up to about 500 m. A voluminous mafic to ultramafic laccolithic layered intrusion (Kakoulima complex) extends northeastwards from Conakry, on the coast, for 50 km and exceeds 1000 m in thickness (Barrère, 1959; Diallo et al., 1992). The emplacement of these sills and the laccolith was controlled by old NW–SE lineaments reactivated during Mesozoic time (Bertrand and Villeneuve, 1989). Dykes, in contrast to sills and laccoliths, are much less frequent in Guinea than in Guyana and only a small N–S swarm was identified in the Bassarides Pan-African belt, west of Fouta Djalon. The major field difference between Guinea and Guyana CAMP formations concerns the volume of preserved magmatic rocks, which are much higher in the former.

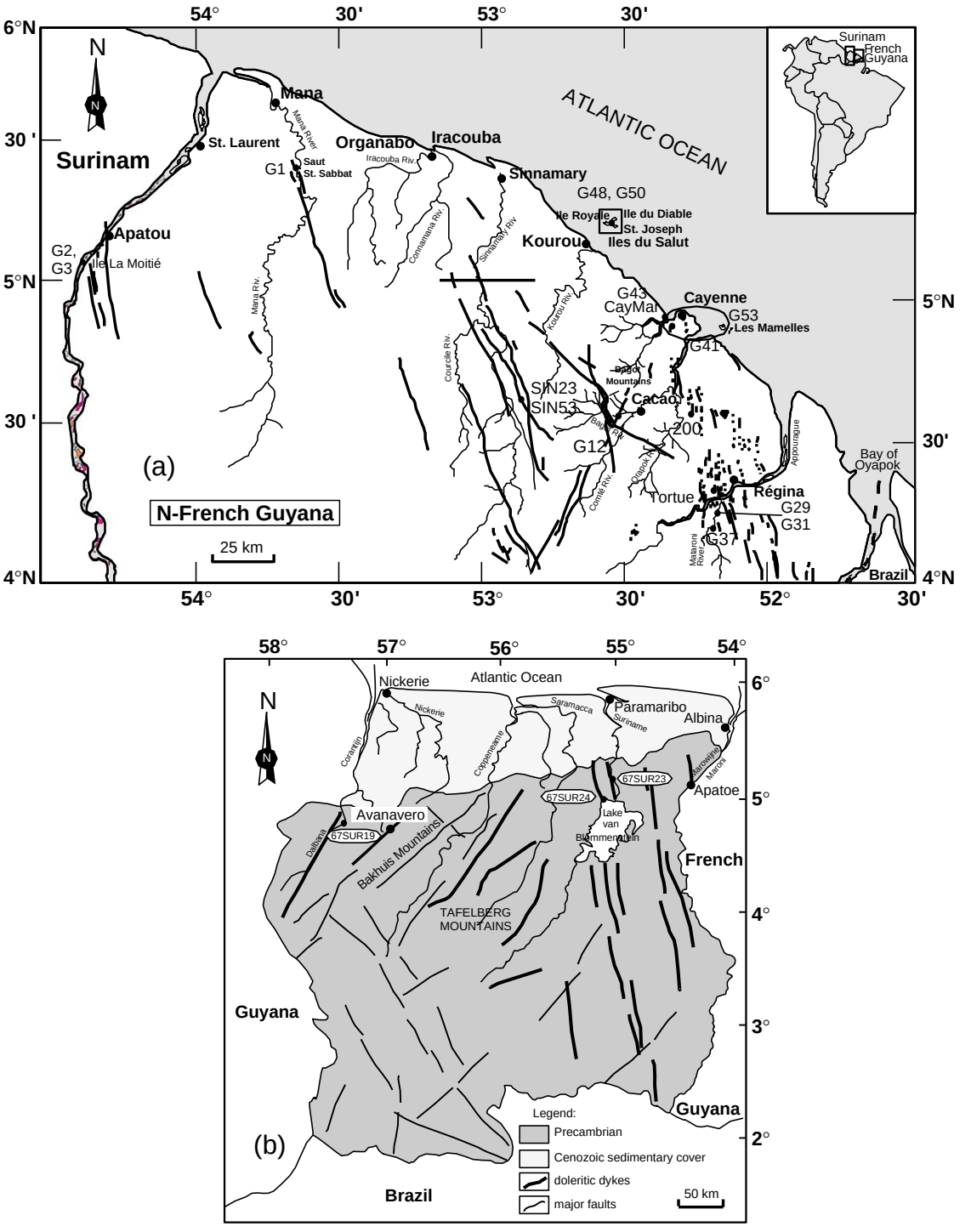

Fig. 2. Sample location map of (a) French Guyana and (b) Surinam, South America. These two regions are referred to as “Guyana” in the text.

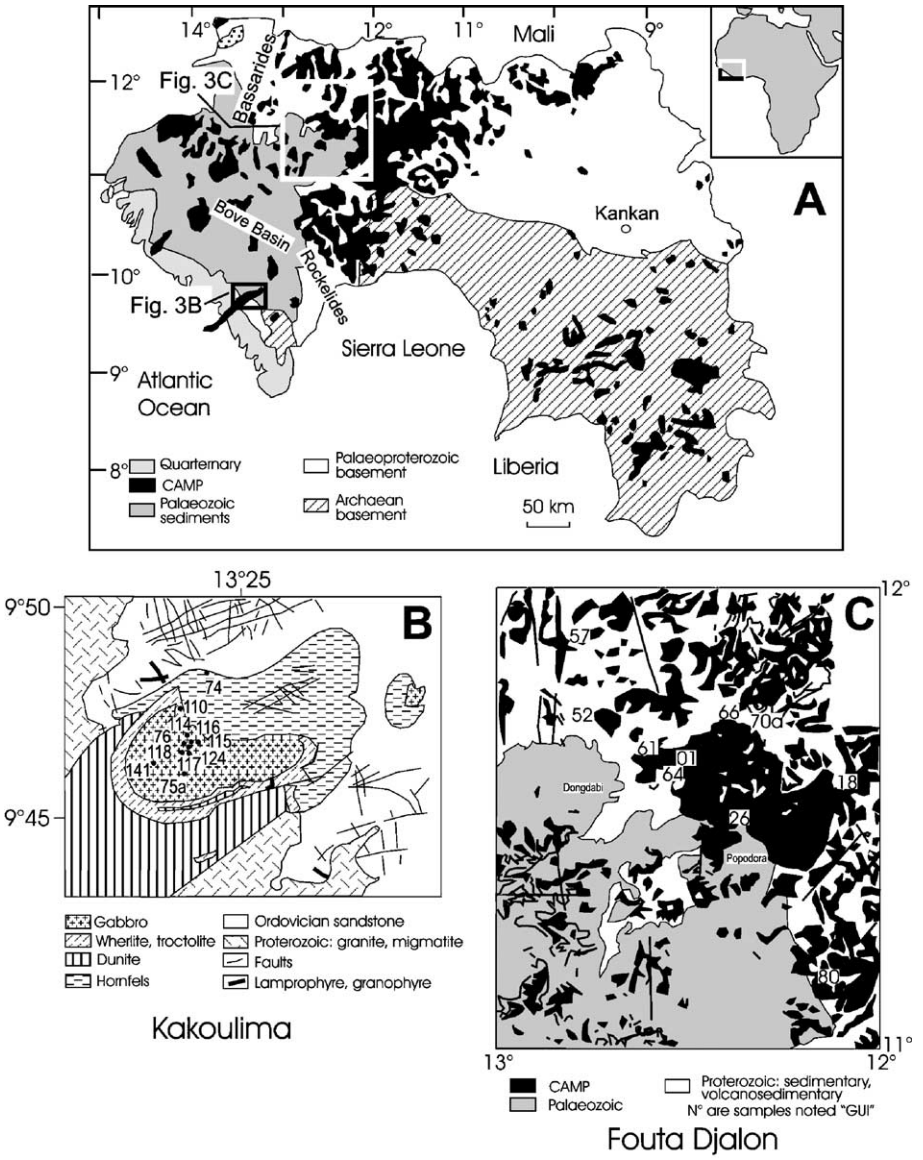

Fig. 3. Geological map of Guinea (A), West Africa (modified after Diallo and Galperov, 1984) and sample locations on Kakoulima laccolithic intrusion (B) and Fouta Djalon sills and dykes (C).

Only a few studies have investigated CAMP geochronology in Guyana and Guinea. The Guyana dyke swarm has been previously dated by the K–Ar method between 206 Ma and 237 Ma (Priem et al., 1968). More recently, a comprehensive $^{40}Ar/^{39}Ar$ study on Guyana and Guinea defined for both regions a magmatic event between 200 Ma and 195 Ma (Deckart et al., 1997). These results, the first relating the age of igneous activity in these countries with CAMP, are concordant with the U–Pb zircon age of 201±1 Ma (Dunning and Hodych, 1990) and plagioclase $^{40}Ar/^{39}Ar$ ages of 200 Ma (Hames et al., 2000) measured in eastern North America, and with the mean age of 199.0±2.4 Ma proposed for CAMP (Marzoli et al., 1999). Younger ages in the range 194–197 Ma recently measured in Guyana, based on a

$^{40}Ar/^{39}Ar$ plagioclase data set affected by excess Ar (Nomade et al., 2002b), are consistent with the youngest data of Deckart et al. (1997) and suggest that secondary magma pulses may have occur in this area of CAMP.

3. Petrographical notes

Dykes and sills from Guyana are relatively homogeneous and range from fine-grained intergranular dolerites to coarse-grained gabbros, depending on the thickness of the dyke and on the position of the sample within it. In all samples, the main phases are calcic plagioclase, augite and to a lesser extent titanomagnetite. Olivine is sporadically present in a few samples. The most differentiated rocks, mainly gabbros, contain pigeonite frequently mantled by augite and interstitial patches composed of late crystallizing micropegmatite enclosing needles of apatite. In some cases, late biotite or amphibole are also present.

Petrographical types are much more varied in Guinea and detailed mineralogical data are given elsewhere (Diallo et al., 1992). This region (including the Freetown layered complex in Sierra Leone) is marked by the exceptional abundance of cumulate rocks, associated with thick intrusive complexes, which are generally not exposed elsewhere in CAMP. The Kakoulima complex is composed of two superposed units: the lower unit, about 230 m thick, consists of layered ultramafic cumulates, which change systematically in mineralogy from dunitic adcumulates (olivine+chromite) at the base to wherlitic cumulates upwards. The wherlites contain cumulus olivine, chromite and poikilitic patches of intercumulus clinopyroxene and, in some cases, interstitial orthopyroxene, biotite or amphibole and, upwards, plagioclase. The upper unit, at least 850 m thick, is composed of massive non-layered gabbros which evolve from olivine–two pyroxenes gabbros at the base to noritic gabbros upwards. Ca-plagioclase and pyroxenes are always the dominant phases. Some horizons of recurrent olivine–gabbros are also observed upwards. These gabbros are free of opaque minerals and present characteristics of cumulates.

The sills from Fouta Djalon are dominantly formed by noritic gabbros or dolerites, depending on their thickness. The thickest sill contains wherlitic cumulates similar to those from the Kakoulima complex. The mineralogy of the gabbros (and dolerites) differs from that observed in Kakoulima by the presence of titanomagnetite and frequent interstitial micropegmatite, biotite and/or amphibole in addition to plagioclase, clinopyroxene and orthopyroxene. Schlieren-like segregations of quartz-diorite pegmatoids may occur locally within the gabbros. The dykes consist of intergranular dolerites containing two clinopyroxenes (augite and pigeonite), plagioclase, titanomagnetite and interstitial micropegmatite and biotite.

The alteration products are variously developed, depending on the samples, and consist of sericite (after plagioclase), serpentine (after olivine), uralite (after pyroxene) and chlorite (after biotite).

The igneous paragenesis observed in dolerites and gabbros, from both Guinea and Guyana, is typical of continental tholeiites (Bertrand, 1991), and is comparable with those described in other CAMP dolerites and gabbros from the four continents concerned (e.g., Weigand and Ragland, 1970; Azambre et al., 1987; Bertrand, 1991; DeMin et al., 2003).

4. Analytical methods

Major and transition elements (Sc, V, Cr, Co, Ni) were analysed by X-ray fluorescence in the University of Lyon (France) for the samples from French Guyana/Surinam and Kakoulima (Guinea) and by ICP-AES in C.R.P.G. of Nancy (France) for the samples of Fouta Djalon (Guinea). Other trace elements were analysed by a VG PlasmaQuad PQ1 ICP-MS at the G.P.I. in the University of Kiel (Germany), from solutions prepared by a standardized digestion with HF–$HClO_4$–aqua regia. For these analyses, the values obtained on international standards like BHVO, BIR, DNC-1, JB-2, NIM-N, UB-N and WS-E are in good agreement with those from Govindaraju (1989), Roelands (1990), Poitrasson et al. (1993), Ionov et al. (1992) and Garbe-Schönberg (1993). The variation coefficient between the measured and recommended values varied between 3% and 10%; however, the standard deviation (1σ) for replicate measurements on the standards range in general from 1% to 7%.

Table 1a
Major and trace element composition of the CAMP tholeiites of Guyana

	G1 dyke	G2 dyke	G3 dyke	G12 dyke	G29 dyke	G31 dyke	G37 dyke	G41 dyke	G43 dyke	G48 sill	G50 sill	G53 dyke	200 dyke	SIN23 dyke	SIN53 dyke	CAYMAR dyke	TORTUE dyke	SUR19 dyke	SUR23 dyke	SUR24 dyke	
Altitude	–	–	–	–	–	–	–	–	–	–	–	–	–	–	–	–	–	–	–	–	Altitude
SiO_2	49.61	50.48	48.72	47.64	49.85	49.41	50.01	49.54	49.47	49.62	48.96	48.90	49.88	49.03	49.41	49.82	49.18	49.05	50.19	49.83	SiO_2
Al_2O_3	13.25	13.91	15.36	13.89	14.30	13.05	13.12	13.69	12.73	14.23	14.03	15.84	14.72	13.72	12.94	13.48	13.29	16.97	14.00	13.34	Al_2O_3
FeO_t	15.50	14.71	13.26	15.78	13.19	15.51	14.55	14.72	15.71	13.39	13.94	11.49	13.70	14.15	15.77	15.00	14.71	13.48	14.86	15.25	FeO_t
MgO	5.36	4.73	6.98	6.02	6.39	5.87	5.85	6.13	5.35	6.65	6.80	7.35	5.17	6.64	5.16	5.49	6.66	4.24	4.64	5.58	MgO
CaO	9.48	9.20	10.91	10.32	10.50	9.98	10.49	10.09	10.16	10.82	10.88	12.60	9.47	10.38	9.24	10.05	10.58	10.10	9.23	9.94	CaO
Na_2O	2.29	2.41	2.11	2.14	2.29	2.23	2.28	2.27	2.25	2.18	2.16	1.94	2.45	2.23	2.49	2.30	2.06	2.44	2.32	2.13	Na_2O
K_2O	0.61	0.75	0.31	0.33	0.52	0.47	0.53	0.41	0.46	0.32	0.31	0.19	0.72	0.42	0.71	0.45	0.34	0.49	0.71	0.51	K_2O
TiO_2	3.30	3.19	2.00	3.43	2.51	2.96	2.65	2.67	3.29	2.37	2.47	1.39	3.27	2.91	3.67	2.87	2.73	2.84	3.41	2.89	TiO_2
P_2O_5	0.36	0.42	0.16	0.24	0.25	0.28	0.27	0.25	0.33	0.23	0.23	0.12	0.41	0.30	0.39	0.30	0.24	0.20	0.43	0.29	P_2O_5
MnO	0.24	0.21	0.19	0.22	0.20	0.24	0.24	0.22	0.23	0.21	0.22	0.19	0.21	0.21	0.23	0.23	0.22	0.18	0.21	0.23	MnO
LOI	0.05	0.08	0.16	0.36	0.06	0.16	0.12	0.19	0.18	0.36	0.31	0.33	0.30	0.15	0.23	0.07	0.13	0.20	0.25	0.12	LOI
Mg#	0.42	0.40	0.52	0.44	0.50	0.44	0.46	0.47	0.42	0.51	0.51	0.57	0.44	0.50	0.41	0.43	0.49	0.40	0.40	0.43	Mg#
Sc	16	15	7	15	12	16	19	13	15	14	15	10	15	12	12	13	18	5	8	18	Sc
V	484	423	442	677	439	529	448	497	534	429	423	327	348	517	476	503	581	485	427	516	V
Cr	68	70	166	64	131	98	68	101	41	135	135	181	90	157	44	74	117	26	64	76	Cr
Co	51	45	49	53	48	52	51	54	50	51	50	49	45	51	54	52	55	46	47	53	Co
Ni	55	66	124	75	80	73	56	78	47	83	87	92	63	95	54	57	78	57	56	66	Ni
Li	9	25	10		9				36	9	8	6	9		14			12	13		Li
Rb	13.9	24.6	8.2	6.8	12.6	12.6	10.7	10.2	10.5	6.9	6.4	4.5	16.8	9.4	17.8	13.2	6.0	13.2	18.4	11.9	Rb
Sr	244	268	222	221	202	221	245	218	260	216	191	184	205	230	386	210	192	255	268	200	Sr
Ba	129	164	57	248	149	143	166	143	121	63	59	45	142	194	218	209	152	103	186	220	Ba
Cs	0.83	3.11	1.19		1.10				1.66	0.20	0.42	0.21	0.42		0.57			0.57	0.83		Cs
Zr	171	280	102	150	171	191	168	157	233	149	134	66	275	183	275	203	157	123	274	182	Zr
Hf	5.01	6.69	2.64		4.49				5.57	3.67	4.01	1.96	6.97		6.43			3.30	6.37		Hf
Nb	15	17	7	11	12	11	14	11	18	10	9	4	20	16	26	11	9	11	18	9	Nb
Y	36	53	23	34	34	40	35	35	45	34	33	21	50	36	43	42	32	29	51	42	Y
Th	1.58	1.89	0.66		1.30				1.44	0.80	0.84	0.37	1.97		1.92			1.28	1.92		Th
U	0.45	0.54	0.21		0.41				0.40	0.21	0.25	0.12	0.61		0.53			0.35	0.57		U
Ta	0.91	0.91	0.37		0.71				0.94	0.55	0.58	0.25	1.19		1.29			0.59	0.94		Ta
La	14.85	18.43	7.49		13.30				16.83	9.51	8.84	4.41	20.15		26.13			11.56	20.08		La
Ce	37.11	48.00	19.42		34.07				43.15	25.29	23.72	11.57	50.71		64.36			29.17	50.39		Ce
Pr	5.60	6.86	2.84		4.80				6.09	3.71	3.90	1.86	7.41		8.73			4.17	7.08		Pr
Nd	25.81	31.47	13.65		22.12				27.92	18.05	18.67	9.17	33.95		38.82			19.31	31.54		Nd
Sm	6.79	8.51	4.05		6.17				7.45	5.15	5.51	2.93	9.12		9.45			5.55	8.55		Sm
Eu	2.26	2.73	1.44		1.98				2.42	1.76	1.78	1.08	2.80		2.94			1.90	2.69		Eu
Gd	7.51	9.59	4.59		6.73				8.29	5.83	6.01	3.51	10.03		10.07			5.91	9.74		Gd
Tb	1.21	1.57	0.76		1.11				1.32	0.99	1.01	0.62	1.60		1.49			0.99	1.50		Tb
Dn	7.02	9.06	4.38		6.63				7.77	5.91	6.08	3.78	9.25		8.21			5.73	8.56		Dn
Ho	1.36	1.81	0.89		1.31				1.54	1.19	1.21	0.77	1.82		1.56			1.11	1.67		Ho
Er	3.82	5.01	2.44		3.71				4.31	3.39	3.41	2.20	5.16		4.29			3.10	4.65		Er
Tm	0.52	0.66	0.33		0.50				0.56	0.45	0.46	0.31	0.69		0.55			0.40	0.62		Tm
Yb	3.39	4.33	2.08		3.22				3.67	2.87	3.05	2.00	4.41		3.47			2.62	3.84		Yb
Lu	0.48	0.60	0.29		0.46				0.51	0.40	0.44	0.29	0.63		0.46			0.36	0.56		Lu
Ga	22.18	27.11	22.91		21.80				26.14	23.07	20.44	18.07	24.48		29.04			26.10	27.37		Ga
Pb	2.28	2.63	1.16		1.94				2.29	1.23	1.44	0.94	2.88		2.37			2.06	3.32		Pb

Oxides in wt.%; trace elements in ppm.

Table 1b
Major and trace element composition of the CAMP samples of Guinea

	Ultramafic cumulates				Gabbroic cumulates										Tholeiites							
	Fouta Djalon		Kakoulima		Kakoulima									Fouta Djalon	Fouta Djalon							
	GUI1 wherlite	GUI64 wherlite	GUI126 dunite	GUI74 wherlite	GUI110	GUI76	GUI114	GUI116	GUI124	GUI117	GUI118	GUI75a	GUI141	GUI61	GUI70A	GUI18 gabbroic sills	GUI26	GUI66	GUI52 doleritic dykes	GUI57	GUI80 Qz-diorite	
Altitude	–	–	0 m	120 m	210 m	440 m	530 m	570 m	630 m	730 m	780 m	945 m	1011 m	630 m	740 m	1015 m	–	–	–	–	–	Altitude
SiO_2	43.22	41.48	41.07	42.11	47.40	50.71	48.17	51.68	50.76	51.58	50.76	51.20	51.14	51.13	51.38	51.91	53.70	51.94	52.18	52.93	57.98	SiO_2
Al_2O_3	4.61	2.67	0.74	3.80	14.14	17.52	14.05	14.52	10.93	15.42	15.28	15.77	15.90	14.30	21.84	15.25	14.24	15.12	14.36	14.76	13.07	Al_2O_3
FeO_t	13.07	14.78	16.34	16.24	9.68	7.43	8.65	8.03	10.87	6.72	7.12	6.73	6.77	8.44	6.77	8.44	10.24	9.67	10.49	10.33	11.70	FeO_t
MgO	34.18	37.70	41.37	33.38	17.61	8.88	16.62	11.09	16.89	11.44	13.45	11.91	10.35	12.83	3.33	8.35	6.88	7.72	7.73	6.92	2.85	MgO
CaO	3.35	2.62	0.10	3.07	9.89	13.36	11.03	12.58	9.05	13.03	11.90	12.70	13.74	11.40	12.47	12.81	10.40	11.94	11.14	11.04	7.25	CaO
Na_2O	0.59	0.21	0.01	0.55	0.85	1.63	0.96	1.36	0.90	1.31	1.04	1.19	1.47	0.89	2.61	1.77	2.19	2.06	2.03	2.06	2.57	Na_2O
K_2O	0.21	0.02	0.02	0.17	0.08	0.11	0.12	0.17	0.08	0.10	0.08	0.11	0.07	0.22	0.40	0.40	0.89	0.40	0.57	0.51	2.10	K_2O
TiO_2	0.40	0.17	0.09	0.39	0.19	0.22	0.24	0.39	0.32	0.24	0.20	0.23	0.30	0.46	0.92	0.73	1.04	0.81	1.12	1.06	1.91	TiO_2
P_2O_5	0.17	0.12	0.00	0.04	0.00	0.00	0.01	0.01	0.01	0.01	0.01	0.01	0.12	0.19	0.20	0.19	0.24	0.17	0.22	0.22	0.41	P_2O_5
MnO	0.20	0.21	0.25	0.24	0.16	0.13	0.15	0.17	0.19	0.15	0.15	0.14	0.13	0.14	0.08	0.15	0.17	0.17	0.16	0.16	0.17	MnO
LOI	1.83	3.98	10.50	0.61	0.10	0.17	0.51	0.16	0.13	0.23	0.27	0.28	0.18	0.09	0.09	0.00	0.00	0.00	0.00	0.95	1.10	LOI
Mg#	0.85	0.84	0.84	0.81	0.79	0.71	0.80	0.74	0.77	0.78	0.80	0.79	0.76	0.76	0.51	0.67	0.58	0.63	0.61	0.58	0.34	Mg#
Sc	16	14		10	23	34	24	38	26	31	28	32	42	38	25	44	43	44	42	41	38	Sc
V	102	81		76	78	116	91	142	120	124	98	113	220	167	199	240	266	265	268	255	323	V
Cr	2974	2400		2252	1102	519	998	499	1139	465	780	695	993	643	35	397	176	262	394	243	11	Cr
Co	131	154		114	61	48	55	39	66	37	44	38	50	59	22	40	40	44	44	43	29	Co
Ni	1293	1268		1033	558	626	311	114	343	121	224	172	159	195	32	77	66	80	100	84	21	Ni
Li					4	4	5	7	4	5	2	5	6	7			16	11			31	Li
Rb	5.7	6.0		4.1	0.8	0.8	1.8	2.4	1.0	1.9	0.6	1.3	1.3	8.6	12.0	13.0	29.9	14.5	18.0	16.0	70.4	Rb
Sr	70	39		82	196	223	171	192	142	190	158	197	197	198	298	198	182	231	177	162	207	Sr
Ba	50	19		42	33	35	35	43	33	30	23	30	38	77	155	110	196	110	131	127	514	Ba
Cs					0.02	0.04	0.05	0.07	0.07	0.04	0.02	0.03	0.04	0.26			1.04	0.37			1.90	Cs
Zr	37	17		34	5	5	11	15	10	9	5	8	10	38	58	63	81	50	89	88	135	Zr
Hf					0.17	0.29	0.29	0.43	0.35	0.25	0.15	0.19	0.28	0.93			2.17	1.34			3.44	Hf
Nb	3	1		3	0	0	1	1	1	1	0	0	0	4	8	9	13	6	8	9	18	Nb
Y	6	3		6	4	5	5	9	6	6	4	13	8	11	16	17	23	17	24	24	39	Y
Th	0.60	0.17		0.45	0.02	0.09	0.15	0.23	0.14	0.15	0.07	0.10	0.10	0.69			2.53	1.12			6.04	Th
U	0.15	0.04		0.11	−0.01	0.06	0.02	0.04	0.06	0.03	0.01	0.01	0.02	0.16			0.58	0.25			1.39	U
Ta	0.14	0.05		0.14	0.01	0.04	0.03	0.04	0.05	0.03	0.01	0.02	0.02	0.19			0.64	0.32			0.97	Ta
La	3.73	1.28		3.40	1.26	1.23	1.99	2.46	1.72	1.58	1.05	2.30	2.07	5.43	9.30	12.69	15.29	7.36	9.69	10.38	26.40	La
Ce	8.30	2.83		7.61	2.60	2.63	4.26	5.77	3.79	3.42	2.22	3.29	4.58	11.62	23.71	27.69	32.52	16.22	24.38	25.13	57.29	Ce
Pr	1.07	0.38		1.01	0.36	0.41	0.58	0.83	0.55	0.48	0.33	0.66	0.66	1.48			3.92	2.09			7.15	Pr
Nd	4.66	1.68		4.43	1.55	1.90	2.40	3.81	2.53	2.08	1.50	3.12	2.97	6.13	9.61	9.36	15.79	8.90	12.60	11.99	28.77	Nd
Sm	1.11	0.42		1.06	0.43	0.73	0.60	1.09	0.84	0.58	0.46	1.02	0.88	1.53	2.56	2.92	3.79	2.35	3.69	3.50	6.59	Sm
Eu	0.36	0.16		0.36	0.30	0.43	0.31	0.48	0.39	0.34	0.28	0.53	0.46	0.59	1.13	0.83	1.17	0.89	1.02	0.98	1.63	Eu
Gd	1.26	0.48		1.15	0.55	0.85	0.74	1.30	1.00	0.79	0.54	1.62	1.10	1.84	2.48	2.74	4.44	2.76	3.58	3.41	7.21	Gd
Tb	0.20	0.08		0.17	0.09	0.15	0.13	0.23	0.18	0.13	0.10	0.26	0.19	0.30			0.68	0.46			1.12	Tb
Dn	1.16	0.48		0.99	0.66	0.99	0.83	1.52	1.15	0.90	0.65	1.62	1.28	1.85	2.49	2.64	4.13	2.84	3.68	3.62	6.54	Dn
Ho	0.23	0.10		0.19	0.14	0.20	0.17	0.31	0.25	0.19	0.13	0.37	0.26	0.38			0.84	0.57			1.32	Ho
Er	0.68	0.29		0.54	0.41	0.59	0.48	0.89	0.73	0.58	0.40	1.01	0.77	1.11	1.36	1.50	2.47	1.66	2.00	2.06	3.81	Er
Tm	0.09	0.04		0.07	0.05	0.10	0.07	0.12	0.12	0.07	0.06	0.12	0.10	0.15			0.34	0.24			0.50	Tm
Yb	0.60	0.27		0.47	0.40	0.61	0.45	0.80	0.76	0.52	0.40	0.70	0.69	1.03	1.25	1.37	2.29	1.55	1.80	1.86	3.28	Yb
Lu	0.09	0.04		0.07	0.06	0.10	0.06	0.12	0.11	0.08	0.06	0.11	0.09	0.15	0.22	0.23	0.33	0.22	0.31	0.33	0.47	Lu
Ga					13.33	14.16	11.55	14.81	10.34	14.11	11.11	13.69	14.75	15.73			18.19	17.95			22.50	Ga
Pb	1.34	0.94		1.00	0.90	2.91	0.68	0.99	1.17	0.63	0.77	0.53	0.62	1.37			4.26	2.19			13.50	Pb

Oxides in wt.%; trace elements in ppm.

Nd, Sr and Pb isotopic analyses have been carried out at the Africa Museum of Tervuren. Nd isotope compositions have been measured after purification using ion exchange resins, on triple Ta–Re–Ta, Sr isotopic compositions on single Ta and Pb isotopic composition on single Re filaments in a Micromass Sector 54 multi-collector mass spectrometer. Repeated measurements of Nd and Sr isotope ratios agreed at better than 0.000015. The used standard NBS987 gave a value for $^{87}Sr/^{86}Sr=0.710260\pm0.000015$ (normalized to $^{86}Sr/^{88}Sr=0.1194$) and the MERCK Nd standard a value $^{143}Nd/^{144}Nd=0.511740\pm0.000015$ (normalized to $^{146}Nd/^{144}Nd=0.7219$). Although Pb measurements usually have a better within-run precision (0.01–0.05%), the mass fractionation factor (between-run error) is known at ±0.1%, which is the error considered in the interpretation. Decay constants used are 1.42×10^{-11} a^{-1} for ^{87}Rb, 6.54×10^{-12} a^{-1} for ^{147}Sm, for $^{235}U=9.8485\times10^{-10}$ a^{-1} and for $^{238}U=1.55125\times10^{-10}$ a^{-1} (Steiger and Jäger, 1977).

5. Geochemistry and isotope geochemistry

5.1. Chemical rock groups

A set of 41 rocks were analysed for major and trace elements (Tables 1a and 1b): 20 doleritic to gabbroic dykes or sills (2 rocks) from Guyana and 21 rocks from Guinea: 2 ultramafic rocks (dunite and wherlite) and 9 gabbros from the Kakoulima complex, 2 wherlites, 5 gabbros, 1 quartz diorite from the Fouta Djalon sills and 2 doleritic dykes from Fouta Djalon. Among them, 19 samples have been analyzed for Sr and Nd isotopes (Table 2) and 17 for Pb isotopes (Table 3).

On the basis of geochemical data and in accordance with the observed petrography, the data set was subdivided into 4 groups. The first group, *Guyana tholeiites*, is represented by gabbros and dolerites from dykes and sills from Guyana. The Guinean samples, which are petrographically more diversified, were

Table 2
Isotopic compositions of Nd and Sr in CAMP samples from Guyana and Guinea

	Sm	Nd	$^{147}Sm/^{144}Nd$	$(^{143}Nd/^{144}Nd)_o$	2σ	$(^{143}Nd/^{144}Nd)_i$	εNd(o)	εNd(i)	T_{DM}	Rb	Sr	$^{87}Rb/^{86}Sr$	$(^{87}Sr/^{86}Sr)_o$	2σ	$(^{87}Sr/^{86}Sr)_i$
Tholeiites (French Guyana/Surinam)															
G1	6.79	25.81	0.159	0.512808	±0.000006	0.512600	3.32	4.28	679	13.91	244.2	0.1649	0.704551	0.000010	0.704082
G3	4.05	13.65	0.179	0.512877	±0.000009	0.512642	4.66	5.10	768	8.20	221.5	0.1071	0.705387	0.000014	0.705082
G43	7.45	27.92	0.161	0.512840	±0.000007	0.512629	3.94	4.84	620	10.48	260.3	0.1165	0.704479	0.000015	0.704148
G48	5.15	18.05	0.173	0.512903	±0.000005	0.512677	5.17	5.78	562	6.85	216.5	0.0916	0.703435	0.000010	0.703175
G53	2.93	9.17	0.193	0.512922	±0.000008	0.512669	5.54	5.63	925	4.49	183.6	0.0707	0.703686	0.000015	0.703485
200	9.12	33.95	0.162	0.512841	±0.000004	0.512628	3.96	4.84	629	16.83	204.5	0.2382	0.704405	0.000011	0.703728
SIN53	9.45	38.82	0.147	0.512803	±0.000006	0.512610	3.22	4.49	575	17.78	385.9	0.1334	0.704494	0.000013	0.704115
SUR19	5.55	19.31	0.174	0.512835	±0.000008	0.512608	3.84	4.43	812	13.22	255.1	0.1500	0.704224	0.000008	0.703798
Tholeiites (Guinea)															
GUI66	2.35	8.90	0.159	0.512497	±0.000008	0.512288	−2.75	−1.80	1527	14.51	231.0	0.1818	0.706745	0.000008	0.706319
GUI52	3.69	12.60	0.177	0.512508	±0.000008	0.512276	−2.54	−2.04	2233	18.00	177.0	0.2943	0.706836	0.000011	0.705999
GUI57	3.50	11.99	0.177	0.512482	±0.000005	0.512251	−3.04	−2.53	2310	16.00	162.0	0.2858	0.707282	0.000010	0.706469
GUI80	6.59	28.77	0.138	0.512290	±0.000009	0.512109	−6.79	−5.30	1520	70.36	206.5	0.9860	0.713525	0.000009	0.710719
Gabbroic cumulates (Guinea)															
GUI76	0.73	1.90	0.232	0.512445	±0.000024	0.512141	−3.76	−4.67	–	0.79	222.8	0.0103	0.706112	0.000011	0.706083
GUI116	1.09	3.81	0.173	0.512366	±0.000023	0.512140	−5.31	−4.69	2538	2.43	192.4	0.0366	0.707461	0.000010	0.707357
GUI118	0.46	1.50	0.186	0.512487	±0.000010	0.512244	−2.95	−2.67	3207	0.55	157.8	0.0101	0.706807	0.000008	0.706778
GUI141	0.88	2.97	0.180	0.512455	±0.000008	0.512220	−3.57	−3.14	2674	1.31	197.5	0.0192	–	–	–
GUI61	1.53	6.13	0.151	0.512455	±0.000008	0.512257	−3.57	−2.41	1429	8.60	197.9	0.1257	0.706554	0.000008	0.706196
Ultramafic cumulates (Guinea)															
GUI1	1.11	4.66	0.145	0.512479	±0.000008	0.512290	−3.10	−1.77	1240	5.73	69.9	0.2400	0.706316	0.000008	0.705641
GUI74	1.06	4.43	0.144	0.512592	±0.000012	0.512403	−0.90	0.44	993	4.10	82.0	0.1450	0.705219	0.000007	0.704808

Sm, Nd, Rb and Sr in ppm. Initial (i) values calculated at 200 Ma, (o) measured.

Table 3
Isotopic compositions of Pb in CAMP samples from Guyana and Guinea

	Th	U	Pb	U/Th	Th/Pb	U/Pb	$^{238}U/^{204}Pb$	$^{235}U/^{204}Pb$	$^{232}Th/^{204}Pb$	$^{206}Pb/^{204}Pb$	$^{207}Pb/^{204}Pb$	$^{208}Pb/^{204}Pb$	$(^{206}Pb/^{204}Pb)_i$	$(^{207}Pb/^{204}Pb)_i$	$(^{208}Pb/^{204}Pb)_i$
Tholeiites (French Guyana)															
G1	1.58	0.45	2.28	0.29	0.69	0.20	12.53	0.09	45.22	18.343	15.524	38.241	17.948	15.505	37.792
G3	0.66	0.21	1.16	0.31	0.57	0.18	11.24	0.08	37.59	18.827	15.653	38.338	18.473	15.635	37.964
G43	1.44	0.40	2.29	0.28	0.63	0.18	11.11	0.08	41.16	18.624	15.512	38.215	18.274	15.495	37.806
G48	0.80	0.21	1.23	0.26	0.65	0.17	10.88	0.08	42.79	18.522	15.530	38.331	18.179	15.513	37.905
G53	0.37	0.12	0.94	0.32	0.40	0.13	8.08	0.06	25.73	18.240	15.481	37.903	17.986	15.469	37.647
200	1.97	0.61	2.88	0.31	0.68	0.21	13.30	0.10	44.63	18.550	15.493	38.097	18.131	15.472	37.653
SIN53	1.92	0.53	2.37	0.28	0.81	0.23	14.26	0.10	53.05	18.504	15.482	38.233	18.055	15.460	37.706
SUR19	1.28	0.35	2.06	0.27	0.62	0.17	10.82	0.08	40.85	18.750	15.572	38.487	18.410	15.554	38.081
Tholeiites (Guinea)															
GUI66	1.12	0.25	2.19	0.22	0.51	0.11	7.16	0.05	33.53	18.620	15.622	38.606	18.394	15.610	38.272
GUI80	6.04	1.39	13.50	0.23	0.45	0.10	6.61	0.05	29.61	18.649	15.671	38.784	18.441	15.660	38.490
Gabbroic cumulates (Guinea)															
GUI76	0.09	0.06	2.91	0.64	0.03	0.02	1.26	0.01	2.03	18.393	15.606	38.368	18.353	15.604	38.348
GUI116	0.23	0.04	0.99	0.18	0.23	0.04	0.03	0.00	0.20	–	–	–	–	–	–
GUI118	0.07	0.01	0.77	0.16	0.09	0.01	0.95	0.01	5.97	18.367	15.573	38.223	18.337	15.571	38.164
GUI141	0.10	0.02	0.62	0.18	0.16	0.03	1.86	0.01	10.49	18.234	15.613	38.264	18.176	15.610	38.160
GUI61	0.69	0.16	1.37	0.23	0.50	0.12	7.32	0.05	32.82	18.447	15.614	38.510	18.216	15.602	38.184
Ultramafic cumulates (Guinea)															
GUI1	0.60	0.15	1.34	0.24	0.45	0.11	6.90	0.05	29.35	18.611	15.633	38.395	18.394	15.622	38.103
GUI74	0.45	0.11	1.00	0.23	0.45	0.11	6.71	0.05	29.58	18.490	15.578	38.494	18.278	15.567	38.200

U, Th and Pb in ppm. Initial (i) values calculated at 200 Ma.

subdivided into three groups: the first two are cumulate groups formed respectively by the *ultramafic cumulates*, composed of the lower ultramafites (dunites and wherlites) from both Kakoulima laccolith and Fouta Djalon sills and by the *gabbroic cumulates* comprising the gabbros from Kakoulima (and one lower gabbro GUI61 from the lower part of a Fouta Djalon sill); the last group, *Guinea tholeiites*, corresponds to the gabbros, diorites and dolerites from sills and dykes from Fouta Djalon.

5.2. Major elements

The studied rocks present contrasting major element behaviour in Guinea and Guyana. The Guyana group is characterized by a Fe-enriched tholeiitic trend whereas the Guinean groups have a less Fe-enriched character. Using the FeO_t/MgO ratio as an index of differentiation, major elements show two distinct trends for cumulate and non-cumulate groups (Fig. 4). The cumulates display a narrow range of FeO_t/MgO ratio (0.38–0.49 in ultramafic and 0.52–0.84 in gabbroic cumulates) and show low TiO_2 concentration (<0.5%), which can be correlated with the absence of Fe–Ti oxides. SiO_2 and Al_2O_3 (Fig. 4a,b), CaO, FeO and MgO (Tables 1a and 1b) concentrations demonstrate the accumulation of olivine–clinopyroxene (ultramafic cumulates) and/or plagioclase (gabbroic cumulates).

The two Guinea and Guyana tholeiitic groups display a larger variation of FeO_t/MgO ratios (ranging from 1.01 to 4.11 and from 1.56 to 3.21, respectively) and distinct major element signatures. *Guinea tholeiites* are Si-rich (SiO_2: 51.4–58.0%), Fe-poor (FeO_t: 6.8–11.7%) and Ti-poor (TiO_2: 0.7–1.1% for basaltic compositions) compared to the Guyana group (SiO_2: 47.6–50.5%, FeO_t: 11.5–15.8%, TiO_2: 2.5–3.5%; Fig. 4 and Tables 1a and 1b). The Ti contents of Guinea and Guyana tholeiites fit the fields of low-Ti and high-Ti continental flood basalts (CFB), respectively (Albarède, 1992).

In all diagrams (e.g., Fig. 4), two Guinean samples, GUI80 and GUI70a, display a particular behaviour.

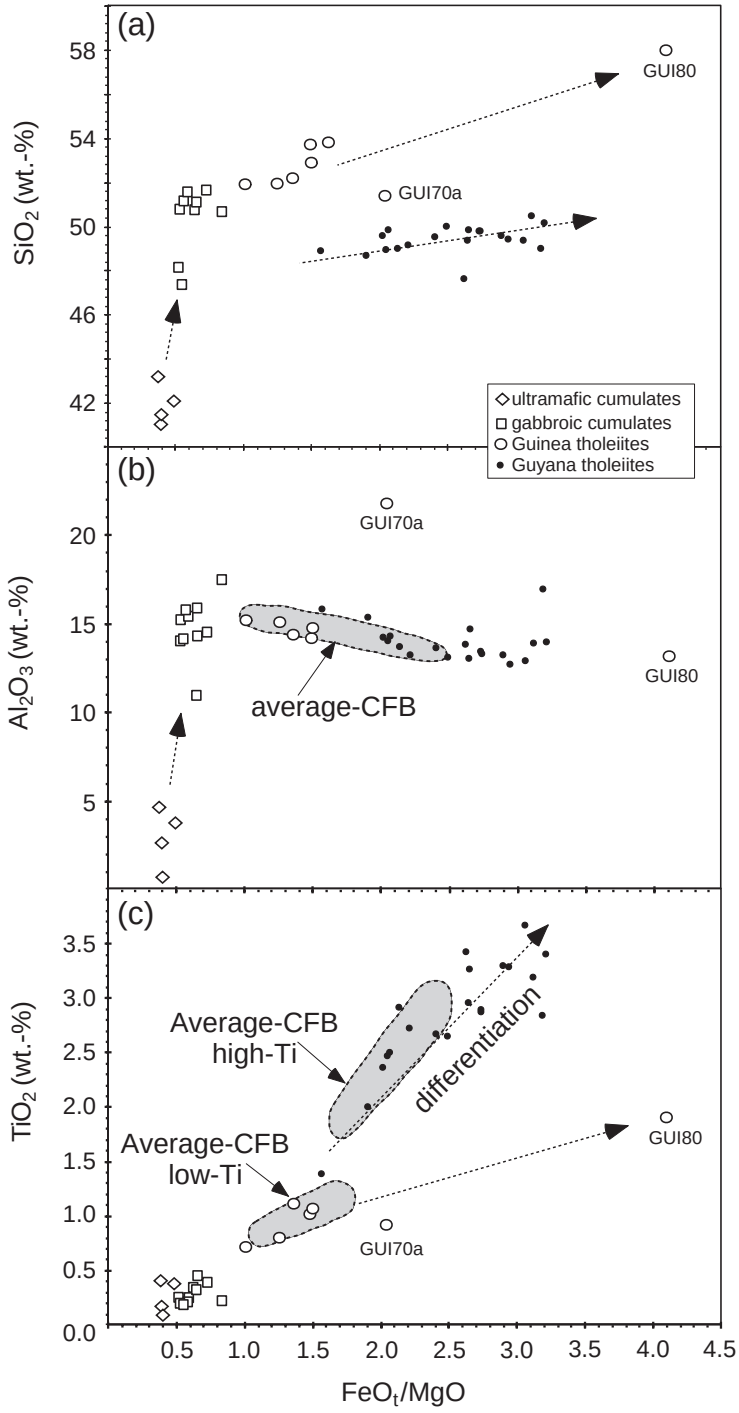

Fig. 4. Major element variations as a function of the FeO_t/MgO ratio (used as the index of differentiation) (a) SiO_2 vs. FeO_t/MgO, (b) Al_2O_3 vs. FeO_t/MgO and (c) TiO_2 vs. FeO/MgO. CFB fields for comparison from Albarède (1992).

The quartz-diorite GUI80 is the most differentiated rock (FeO_t/MgO=4.1 with SiO_2=58.0%), but retains the overall trend of the *Guinean tholeiites*. Sample GUI70a, although classified in the same group, contains patches of cumulate plagioclase and represents therefore a crystal-laden liquid, indicated, for example, by its high Al_2O_3 content (Fig. 4b).

5.3. Trace elements

The chondrite-normalized rare earth element (REE) diagram of the *Guyana tholeiites* (Fig. 5a) shows variably enriched patterns ($(La/Yb)_n$: 1.5–5.1), lacking or showing only a very weak (in the most enriched samples) negative Eu anomaly. This enriched character is also displayed in the trace element spidergrams normalized to the average mid-ocean ridge basalts (MORB) (Fig. 6a) where a continuous increase in the element abundance occurs from right to left, in agreement with the incompatible character of these elements. No Nb–Ta anomaly is observed. Positive to negative Sr anomalies and a slight positive Ti anomaly already mentioned are characteristic of the *Guyana tholeiites*. The Sr and very weak Eu depletions indicate the low-P fractionation of plagioclase. Sample G53, with the lowest concentration in

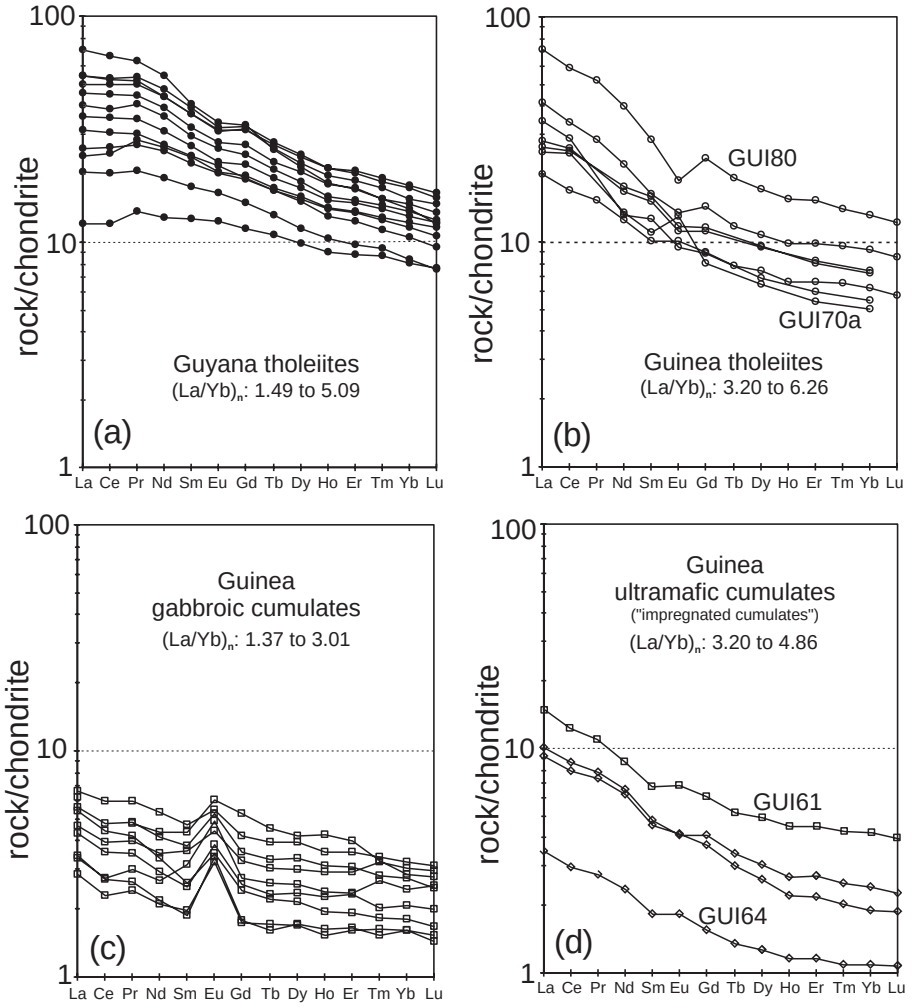

Fig. 5. Chondrite normalized (Taylor and McLennan, 1985) REE patterns of (a) Guyana tholeiites, (b) Guinea tholeiites, (c) Guinea gabbroic cumulates and (d) Guinea impregnated cumulates (ultramafic cumulates+gabbroic cumulate GUI61).

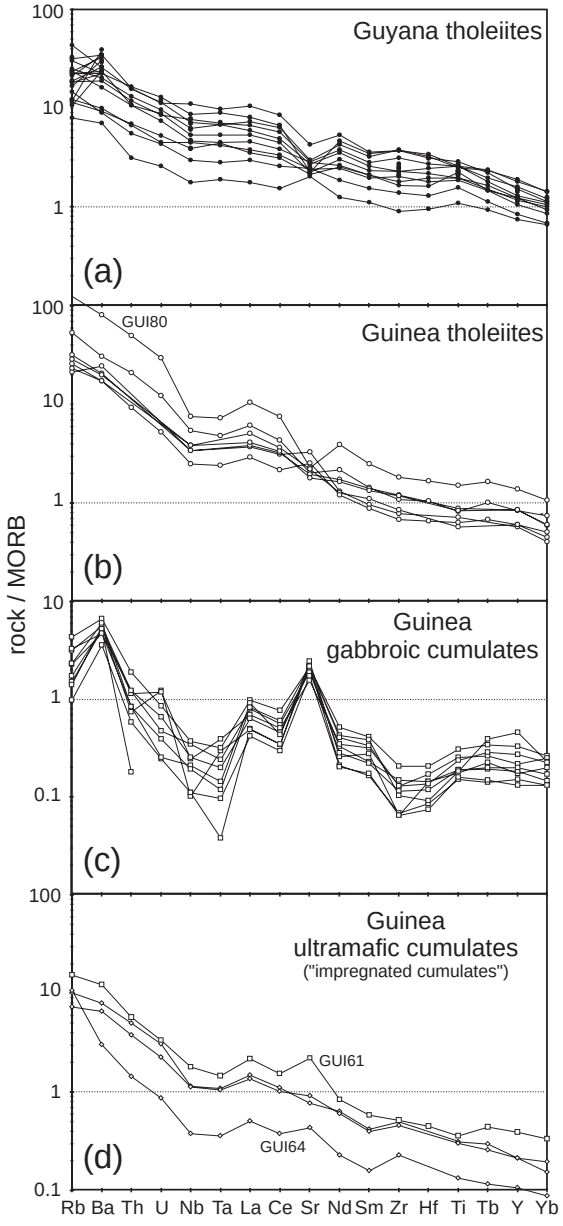

Fig. 6. N-MORB normalized (Sun and McDonough, 1989) trace element patterns of (a) Guyana tholeiites, (b) Guinea tholeiites, (c) Guinea gabbroic cumulates and (d) Guinea impregnated cumulates (ultramafic cumulates+gabbroic cumulate GUI61).

trace elements and a positive anomaly in Sr, has a weak plagioclase cumulate character. The erratic variability observed for Rb and, to lesser extent, for Ba and K (not shown) in some samples is probably due to slight weathering of these samples (Fig. 6a). Nevertheless, this alteration is minor and did not affect the overall trace element patterns.

On average, *Guinea tholeiites*, from Fouta Djalon, have slightly more light REE (LREE) enriched patterns ($(La/Yb)_n$: 3.2–6.3) and more pronounced Eu anomalies than Guyana tholeiites (Fig. 5b). The plagioclase-laden character of the sample GUI70a is attested by a clear positive Eu anomaly. The Guinea tholeiites are also more enriched in LILE such as Rb, Ba, K and in Th compared to high field strength elements (HFSE) such as Nb, Ta, Ti, and display a pronounced Nb–Ta negative anomaly but no Ti anomaly (Fig. 6b).

The *gabbroic cumulates*, from Kakoulima, have typical REE patterns (Fig. 5c) for such rocks: low global REE abundances, low $(La/Yb)_n$ ratios (from 1.4 to 3.0) and large positive Eu anomalies. The same character is shown by the trace element spidergrams (Fig. 6c), which display a large positive Sr anomaly correlated to the Eu anomaly in response to plagioclase accumulation. However, as with the *Guinea tholeiites*, these cumulates possess a well-marked negative Nb–Ta anomaly and are enriched in LILE.

The *ultramafic (wherlite) cumulates*, from both Kakoulima and Fouta Djalon, and the gabbroic cumulate from Fouta Djalon GUI61 share common trace element patterns, with mixed features of *Guinea tholeiites* and Kakoulima gabbroic cumulates. Compared to the latter, they have lower HREE but higher LREE abundances (except GUI64), with $(La/Yb)_n$ ratio from 3.20 to 4.86, no Eu anomalies (Fig. 5d), no or slight positive Sr anomalies, and higher LILE abundances (Fig. 6d). These abundances suggest that these cumulates contain a significant amount of trapped liquid and can be called “impregnated cumulates”. Sample GUI64, with its low REE abundances, should be the least impregnated among this group of wherlitic cumulates.

5.4. Nd–Sr–Pb isotopes

Measured and initial (back-calculated to 200 Ma) isotopic ratios are reported in Table 2 (Nd–Sr isotopes) and Table 3 (Pb isotopes). Regarding the entire data set, Nd and Sr initial ratios vary considerably: εNd_i from +5.8 to −5.3, $(^{87}Sr/^{86}Sr)_i$ from 0.703175 to 0.710719, whereas Pb initial ratios are

less variable, $(^{206}Pb/^{204}Pb)_i$, $(^{207}Pb/^{204}Pb)_i$ and $(^{208}Pb/^{204}Pb)_i$ ranging from 17.95 to 18.47, from 15.46 to 15.66 and from 37.65 to 38.49, respectively.

Nd and Sr isotope compositions differ strongly between Guyana and Guinea. Guyana tholeiites have radiogenic Nd compositions (εNd_i from +5.78 to +4.28), displaying a slight inverse correlation with (FeO_t/MgO) ratio (Fig. 7a), and unradiogenic Sr compositions, $(^{87}Sr/^{86}Sr)_i$ varying from 0.703175 to 0.705082. They lie in the depleted quadrant (except sample G3 which may have suffered some Rb–Sr mobility) of the Nd–Sr isotope diagram and display a slight inverse correlation between the two isotopes (Fig. 8a). In contrast, Guinea samples show a wider isotopic range and lie mainly in the enriched quadrant: εNd_i and $(^{87}Sr/^{86}Sr)_i$ vary from +0.44 to −5.30 and from 0.704808 to 0.710719, respectively, and are strongly inverse correlated. The impregnated wherlitic cumulates have the least enriched signature, sample GUI74 being close to the bulk earth (BE) composition. Gabbroic cumulates and non-cumulate rocks are broadly in the same range (εNd_i from −2.41 to −4.69 and from −1.8 to −5.3, $(^{87}Sr/^{86}Sr)_i$ from 0.706083 to 0.707357 and from 0.705999 to 0.706469, respectively, except the most differentiated quartz-diorite GUI80 which has a higher $(^{87}Sr/^{86}Sr)_i$ ratio of

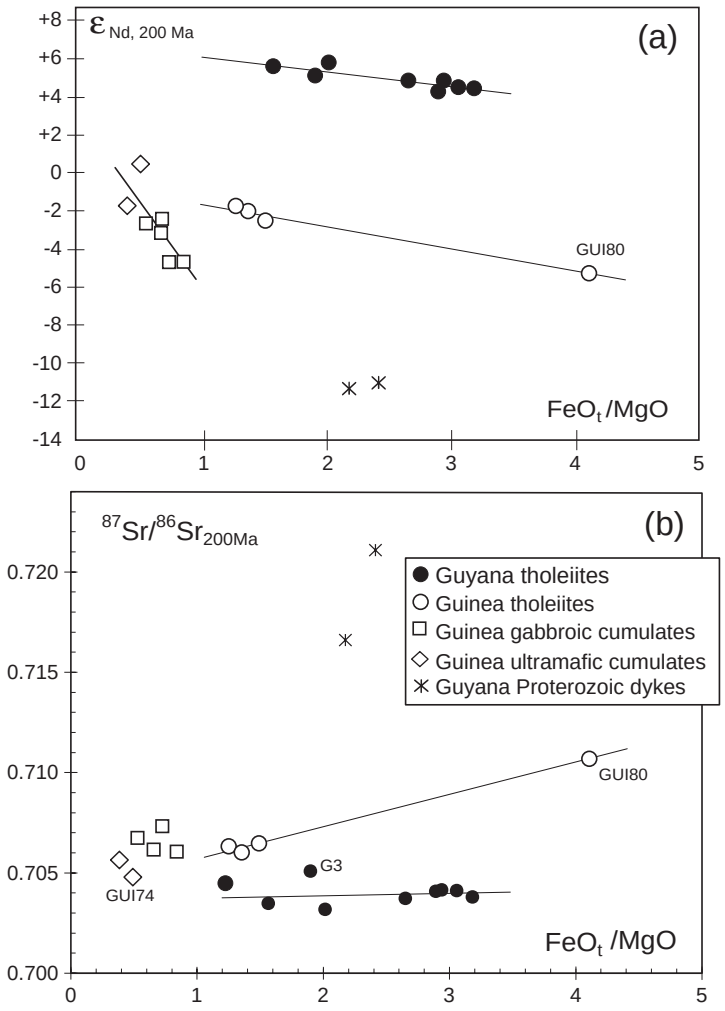

Fig. 7. (a) $\varepsilon Nd_{(i)}$ vs. FeO_t/MgO diagram for Guyana and Guinea CAMP tholeiites. (b) $^{87}Sr/^{86}Sr_{(i)}$ versus FeO_t/MgO. For comparison, both diagrams show two Proterozoic Guyana dolerites.

0.710719) (Fig. 8a). For both cumulate and non-cumulate rocks, Sr and Nd initial ratios are correlated and inverse correlated, respectively, with (FeO_t/MgO) ratio (Fig. 7a and b).

Guyana Pb initial ratios, ($^{206}Pb/^{204}Pb)_i$, ($^{207}Pb/^{204}Pb)_i$ and ($^{208}Pb/^{204}Pb)_i$, range from 17.948 to 18.473, 15.460 to 15.647 and 37.647 to 38.081, respectively (Table 3, Fig. 8b–d). The entire Guinea samples share similar ($^{206}Pb/^{204}Pb)_i$ ratios, ranging from 18.176 to 18.441, but are more radiogenic in ^{207}Pb (($^{207}Pb/^{204}Pb)_i$ from 15.567 to 15.660) and in ^{208}Pb (($^{208}Pb/^{204}Pb)_i$ from 38.103 to 38.490). The cumulates are the least and the quartz-diorite the most radiogenic in ^{207}Pb and ^{208}Pb.

Compared to other CAMP occurrences, the Nd–Sr isotope ratios from Guyana and Guinea cover nearly the whole compositional range observed throughout the province (Fig. 9). More specifically, the Guyana

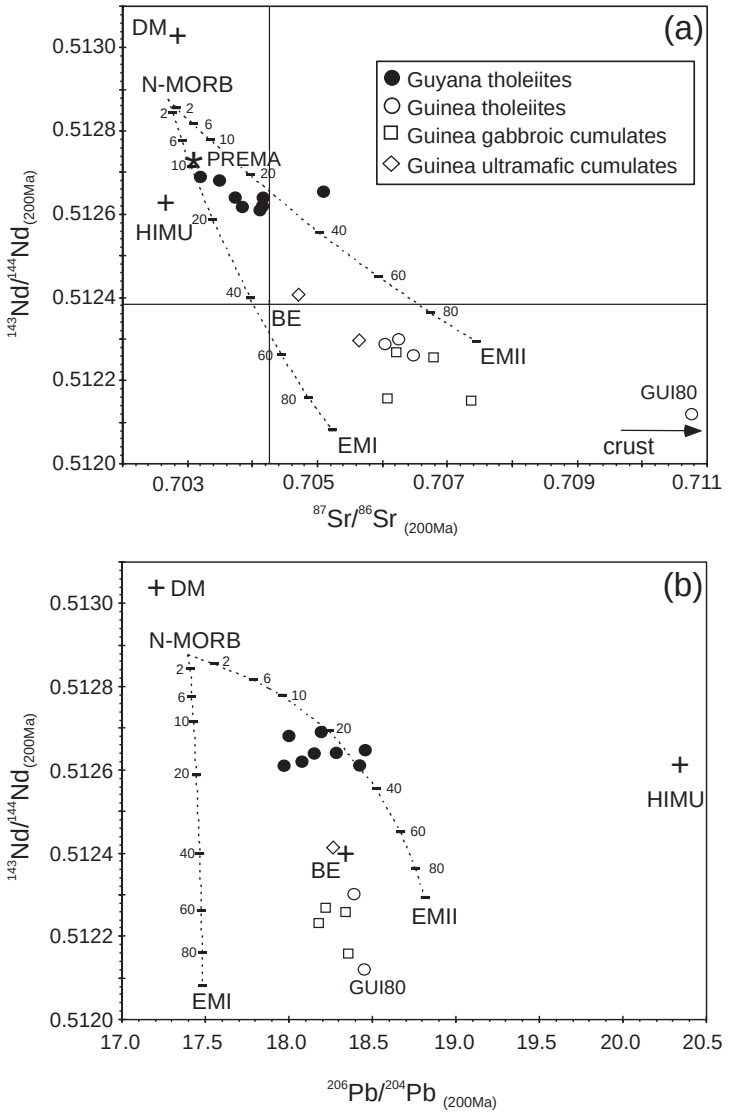

Fig. 8. Initial (200 Ma) isotope characteristics of Guyana and Guinea samples. (a) $^{143}Nd/^{144}Nd$ versus $^{87}Sr/^{86}Sr$, (b) $^{143}Nd/^{144}Nd$ versus $^{206}Pb/^{204}Pb$, (c) $^{207}Pb/^{204}Pb$ versus $^{206}Pb/^{204}Pb$ and (d) $^{87}Sr/^{86}Sr$ versus $^{206}Pb/^{204}Pb$. The diagram shows mixing lines with percentages of mixing between N-MORB and EMI or EMII end-members.

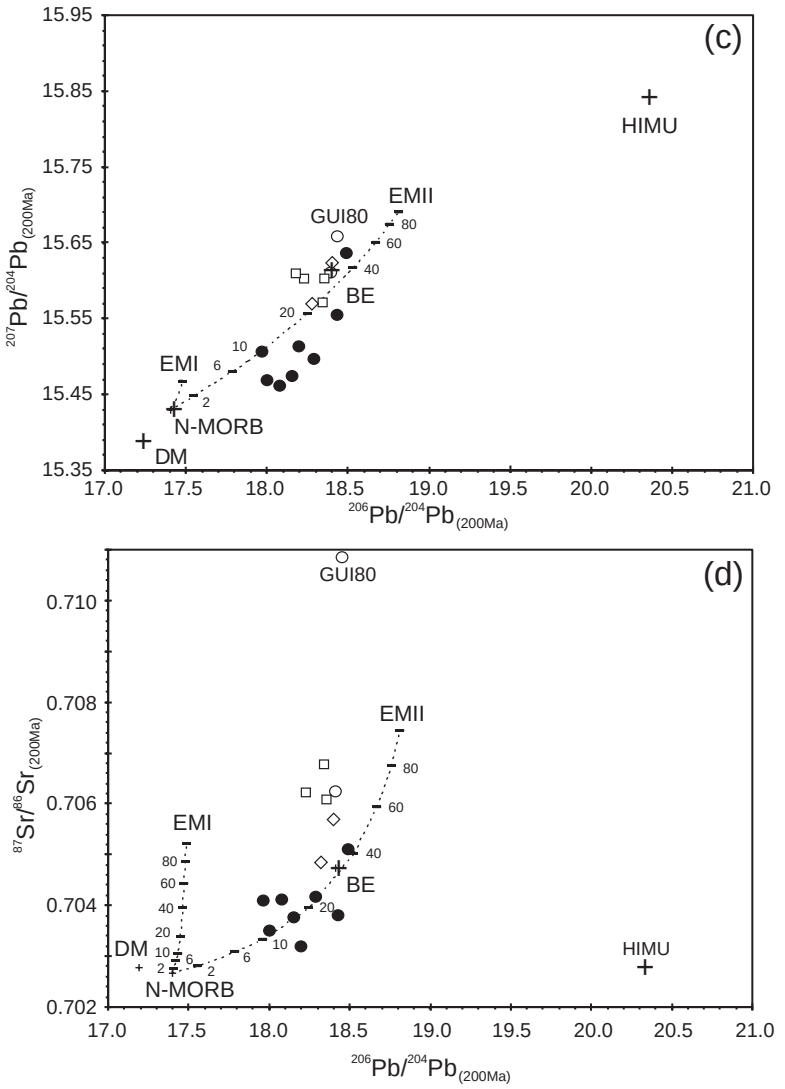

Fig. 8 (*continued*).

tholeiites match the field of high-Ti compositions documented in Liberia (Dupuy et al., 1988) and Brazil (DeMin et al., 2003), whereas Guinea samples (including cumulates and tholeiites) match the field of low-Ti compositions more widely observed in North America (Pegram, 1990), Brazil (DeMin et al., 2003), Liberia (Dupuy et al., 1988), Iberia (Alibert, 1985; Cebriá et al., 2003) and France (Jourdan et al., 2003). Guyana and Guinea samples are therefore good representatives for assessing the petrogenesis and origin of CAMP.

6. Discussion and interpretations

6.1. Contrasting compositions in Guinea and Guyana: crustal contamination or mantle source differences?

It has been stressed that Guinea and Guyana tholeiites have contrasting compositions in respect of their major and trace elements and their radiogenic isotopes. These differences broadly match those characterizing low-Ti and high-Ti groups,

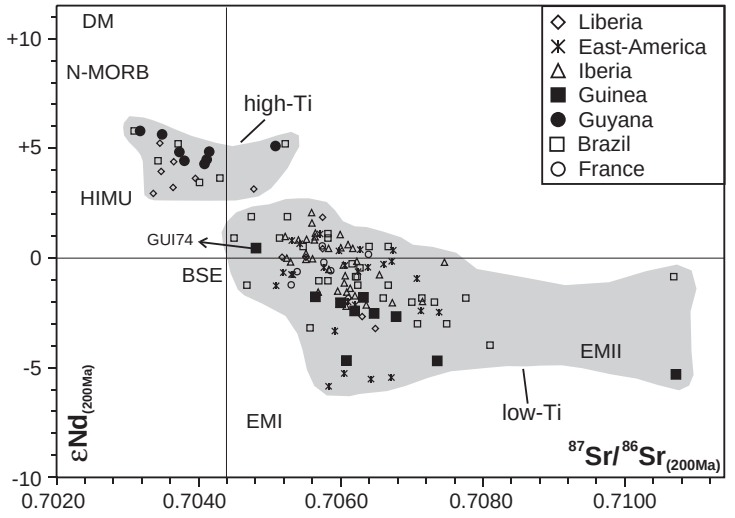

Fig. 9. Initial εNd versus $^{87}Sr/^{86}Sr$ isotope variations using the available data set of CAMP tholeiites. Iberia (Alibert, 1985; Cebriá et al., 2003), Brittany (Jourdan et al., 2003), Liberia (Dupuy et al., 1988), East North America (Pegram, 1990; Heatherington and Mueller, 1991), Brazil (DeMin et al., 2003), Guyana and Guinea from this work. The respective fields of low- and high-Ti CAMP are shaded.

respectively, at the scale of the entire CAMP. As a whole, the Guinea (and low-Ti CAMP) group mainly differs from the Guyana (and high-Ti CAMP) group by higher SiO_2 and lower FeO and TiO_2 contents (Fig. 4), enrichment in LILE, negative Nb–Ta anomalies (Fig. 6), lower $(^{143}Nd/^{144}Nd)_i$ and higher $(^{87}Sr/^{86}Sr)_i$ ratios (Fig. 9). The questions that arise are whether these characteristics reflect those of the mantle sources and their melting conditions and how far crustal assimilation processes have contributed to the observed differences. These major questions on CFB genesis have long been debated and are still unresolved. Concerning CAMP, there is a quasi-consensus for the prevalent low-Ti group being derived from an enriched heterogeneous (probably lithospheric) mantle source, without denying the additional effects of crustal contamination in some cases (Bertrand et al., 1982; Alibert, 1985; Dupuy et al., 1988; Pegram, 1990; Bertrand, 1991; Heatherington and Mueller, 1999; Cebriá et al., 2003; DeMin et al., 2003). This study offers the opportunity to re-evaluate this assessment by comparing the low-Ti (Guinea) with the high-Ti (Guyana) features. The purpose of this section is not to discuss the details of possible crustal contamination processes (developed in the next section), but rather to evaluate whether such processes have modified the chemical signatures of the low-Ti group beyond the point where they can be used as tracers of mantle source compositions.

There is evidence that the compositions of the Guinea (and low-Ti CAMP) group are unlikely to derive from those of Guyana (and high-Ti CAMP) group through crustal contamination processes. In fact, they do reflect different mantle sources and possibly different conditions of melting:

– If the low-Ti group was derived from crustal contamination of the high-Ti group, one would expect that most CAMP magmas should have been contaminated throughout the entire province, except for some, but still not all, dykes in the narrow area formed by coastal Guyana, Liberia and Cassipore in Brazil. Such an hypothesis is unlikely and not supported by any specific geodynamic setting in this area that would particularly prevent the magmas from contamination here rather than elsewhere: Guyana and Cassipore dykes are intruded at the edge of the Amazon craton, whereas the low- and high-Ti Liberia dyke swarm intruded across the West African craton and the Rockelides Pan-African belt. Other low-Ti sills and dykes also straddle the West African craton and the juxtaposed mobile belt and Bove Basin, in Guinea, or intrude equally cratons (e.g., Brazil, Taoudenni) and

Caledonian–Hercynian belts (e.g., eastern North America).

- Most of the differentiation trends based on major elements (e.g., Fig. 4) point to two distinct series for low-Ti and high-Ti groups. Guinea tholeiites are systematically silica-rich and Fe–Ti-poor, compared to Guyana tholeiites, whatever their degree of differentiation, suggesting that they may have been produced by melting under lower pressure, i.e., at shallower depth than Guyana tholeiites (Klein and Langmuir, 1987), rather than through crustal contamination.
- Regarding the Nd–Sr isotope plot (Fig. 9), the distribution of the density of the points, based on ~130 measurements, calls for two distinct fields, corresponding to the low- and high-Ti groups, respectively, separated by a modest but significant gap, without the compositional continuum which would be expected if the low-Ti group had derived from the high-Ti group through crustal contamination.
- Low-Ti CAMP lava-flows from Morocco with composition of primary magma, and therefore free from crustal contamination (e.g., sample MA1137, Bertrand et al., 1982), match the enriched isotopic compositions of the low-Ti group ($(^{87}Sr/^{86}Sr)_i$: 0.706547, εNd_i: −0.31, H.B., unpublished), demonstrating that radiogenic Sr and unradiogenic Nd may reflect the mantle source composition of low-Ti CAMP magmas. On the other hand, initial $^{187}Os/^{188}Os$ ratios close to the value of the primitive upper mantle recently measured on the least differentiated low-Ti tholeiites from Iberia (Rapaille et al., 2003) rule out significant contamination by continental crust for these samples, reinforcing the significance of their isotopic composition in terms of mantle source signature.
- LILE/HFSE enrichment and Nb–Ta anomalies are specific features of Guinea and low-Ti CAMP group, but cannot unequivocally discriminate between mantle source enrichment and crustal contamination processes. However, the presence of these features in the Guinea ultramafic cumulates (Fig. 6) and in the rocks from Morocco and Iberia quoted above, unsuspected to have been contaminated, is an argument in favor of a source signature.

This network of facts supports the derivation of Guinea and other low-Ti CAMP magmas from an enriched and probably heterogeneous mantle source, distinct from that generating the Guyana high-Ti magmas. We consider the wherlitic cumulate GUI74 as the best proxy for the isotopic composition of the primary magma and mantle source in Guinea. It is noteworthy that this composition broadly corresponds to the upper left corner of the low-Ti field from which most Nd–Sr trends are rooted (Fig. 9).

6.2. Evolution of the magmas in Guyana and Guinea: contrasting roles of the continental crust

The differentiation trends defined by major elements (Fig. 4) and the REE patterns (Fig. 5) of the Guinea and Guyana tholeiites indicate that the magmas have undergone early low-pressure crystal fractionation. This process has been more pronounced in Guinea than in Guyana, as attested by the abundance and the compositional range of the cumulates, the thickness of the sills from Fouta Djalon and of the Kakoulima laccolith, the petrographic evolution up to quartz-diorites and the wider range of differentiation index (e.g., FeO_t/MgO).

However, the existence of large magma reservoirs within the continental crust (thick sills and laccolith) may also promote magma–crust interactions. These may have been more important in Guinea than in Guyana (where mainly dyke swarms are observed) and may have contributed to the petrographic and geochemical evolution observed. The large dispersion of the Guinea (and low-Ti CAMP) data in the Nd–Sr isotope plot (Fig. 9) indicates, at least for the most extreme compositions, that some crustal contamination has taken place. Moreover, the correlation and the inverse correlation observed between the FeO_t/MgO ratio and $(^{87}Sr/^{86}Sr)_i$ and εNd_i, respectively, for the Guinea suite (Fig. 7a,b) may suggest combination of assimilation and crystal fractionation (AFC) processes (De Paolo, 1981).

The Nd–Sr isotope signatures of Guyana tholeiites (and high-Ti group) are much less variable and mostly depleted (Fig. 9), supporting less, if any, crustal contamination. However, εNd_i is slightly inversely correlated with the FeO_t/MgO ratio (Fig. 7a) in accordance with an AFC process, although this is

not observed in the pattern of $(^{87}Sr/^{86}Sr)_i$ vs. FeO_t/MgO ratios (Fig. 7b).

In order to quantify the combination of crystal fractionation and crustal assimilation, AFC process has been modeled for Nd and Sr isotopes for both the Guinea and Guyana suites, using as contaminants examples of the regional upper crust, i.e., a granodiorite from the Guinea Birimian basement (Boher et al., 1992) and a Proterozoic dolerite from Guyana (Deckart, 1996), respectively (Fig. 10). Taking the regional geology into account, the West African craton (Palaeoproterozoic or Archaean) is favoured as crustal contaminant and not the Pan-African belts, as T_{DM} model ages for Guinea CAMP tholeiites vary between 1000 and 1500 Ma (mean: 1342±203 Ma), which constitute minimum ages for the bulk contaminant. A larger effect on ^{207}Pb than on ^{206}Pb (Fig. 8c) also implies an old contaminant, as the ^{235}U abundance is very low during the Phanerozoic. A Birimian crust (ca. 2.1 Ga; Liégeois et al., 1991; Boher et al., 1992) is favoured, which should be felsic rather than mafic, since mafic mantle-derived rocks have too high $^{143}Nd/^{144}Nd$ ratios at 200 Ma (mean of 0.5127; Abouchami et al., 1990). The chosen starting compositions for AFC modeling were the most isotopically primitive samples, i.e., samples GUI74 and G48. The Guyana suite fits using a ratio rate of assimilation/rate of fractional crystallization of r=0.1, indicating an extremely weak assimilation, which could account for the slight inverse correlation between $(^{143}Nd/^{144}Nd)_i$ and $(^{87}Sr/^{86}Sr)_i$ ratios. Applying a simple two-component mixing on Guyana magmas, the mixing curve would indicate a crustal contaminant involvement of under 4%. In Guinea, almost the entire range of isotopic compositions of those samples is correctly fitted by an AFC process controlled by a higher rate of assimilation (r=0.3). The only exception is the most differentiated quartz-diorite (GUI80) which may require a different upper crust contaminant. AFC modeling using lower crust compositions as contaminants failed to accommodate the data. These comparative AFC modeling highlight, as mentioned above, the more intense magma–crust interactions in Guinea, in accordance with the geological setting, i.e.,

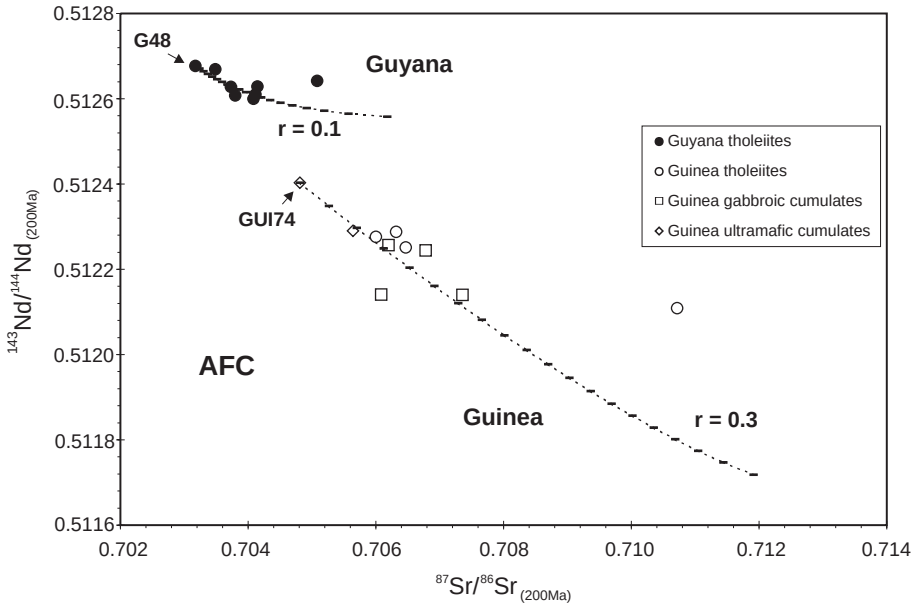

Fig. 10. Combined assimilation-fractional crystallization (AFC, De Paolo, 1981) modeling of $(^{143}Nd/^{144}Nd)_i$ vs. $(^{87}Sr/^{86}Sr)_i$ for Guyana and Guinea samples with Guyana Proterozoic ($(^{87}Sr/^{86}Sr)_{200}$=0.719879, Sr=166 ppm, $(^{143}Nd/^{144}Nd)_{200}$=0.511811, Nd=28.87 ppm, sample G9, Deckart, 1996) and Guinea Birimian ($(^{87}Sr/^{86}Sr)_{200}$=0.713093, Sr=525 ppm, $(^{143}Nd/^{144}Nd)_{200}$=0.510959, Nd=18.25 ppm, sample G9, Boher et al., 1992) contaminants. r=mass assimilation rate/fractional crystallization rate. Curves were calculated with 5% steps of F (fraction of melt remaining). Starting uncontaminated magmas are samples G48 and GUI74 for Guyana and Guinea, respectively (with Nd and Sr concentrations for the starting material in Guinea of 10 ppm and 200 ppm). The bulk distribution coefficients for Nd and Sr were taken as 0.15 and 0.95.

greater volumes of magmas stored in crustal reservoirs and a longer residence time of these magmas within the crust, allowing them to be contaminated as they differentiate. These processes are likely to contribute to the fan-like dispersal of the Nd–Sr isotope ratios away from sample GUI74 in Guinea, as often observed for other low-Ti CAMP (Fig. 9).

The evolution of the magmas in Guyana has also been tentatively modeled through trace elements compositions, combining ratios of very incompatible elements (VICE, such as Th, Nb, LREE), moderately incompatible elements (MICE, e.g., HREE) and compatible elements (CE, e.g., Ni). Ratios of very incompatible elements (VICE/VICE) are invariant either during fractional crystallization or during equilibrium partial melting: for example, Guyana tholeiites show a constant Th/Nb ratio independent of Ce content (Fig. 11a), confirming that these types of ratios can be considered as approaching that of the mantle source (see next section).

In contrast, the Th/Yb ratio (VICE/MICE) displays a positive correlation with Ce, which underlines the role of partial melting in magma genesis (Fig. 11a). Simple crystal fractionation and AFC differentiation processes are also reported, confirming former isotope results by showing that a slight AFC-type process possibly has been involved in magma genesis. This conclusion is strengthened by the Ce vs. Ni diagram (VICE vs. CE; Fig. 11b): fractional crystallization fails to explain the strong enrichment of Ce as Ni concentration decreases, as it is observed in Guyana tholeiites. But, applying the same AFC-process as previously modeled for isotopes (r=0.1) on a ca. 15% partial melt in magma generation accounts for the observed Ce enrichment. The sample G53, among the least contaminated according to isotopes (Fig. 10), would require a very limited amount of fractional crystallization without AFC-type contamination. These considerations indicate that the Guyana basaltic dykes are mantle-derived partial melts with limited effects of a possible combination of AFC and simple fractional crystallization.

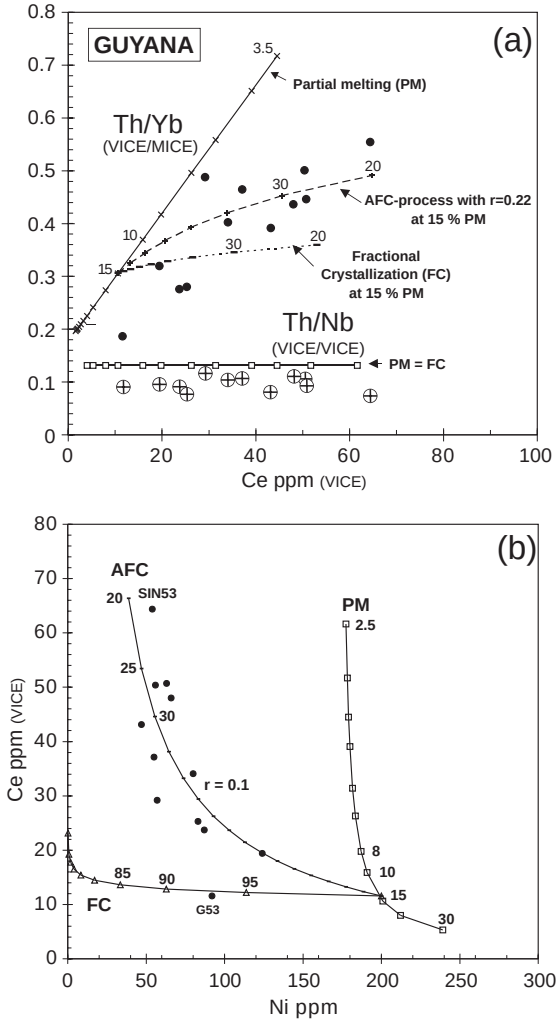

Fig. 11. Partial melting, fractional crystallization and AFC processes modeling for Guyana tholeiites. (a) Th/Yb (VICE/MICE) ratio and Th/Nb (VICE/VICE) ratio vs. Ce (VICE), (b) Ce (VICE) vs. Ni (CE). VICE=very incompatible element; MICE=moderately incompatible element; CE=compatible element as proposed by Hofmann and Jochum (1996). The curves have been calculated with the following initial concentrations (primitive mantle, Hofmann, 1988) and K_d values: Ce: 1.6011 ppm, 0.001; Nb: 0.6175 ppm, 0.001; Th: 0.0813 ppm, 0.001; Yb: 0.4144 ppm, 0.1; Ni: 2080 ppm, 12. Ticks on the different curves correspond to F (=fraction of melt produced for partial melting, or remaining for fractional crystallization and AFC processes, respectively).

6.3. CAMP mantle sources and geodynamical implications

As discussed above, despite clear evidence of crustal contamination, the magma–crust interactions did not modify the Sr and Nd isotope signatures to a point preventing their use as tracers of mantle source compositions in both Guyana and Guinea. This section tentatively discusses the issue of the nature, location and significance of possible mantle compo-

nents involved at the origin of these magmas, from radiogenic isotope systematics and trace element ratios. VICE/VICE ratios which are invariant either during fractional crystallization and partial melting (e.g., Fig. 11a) characterize magmatic rock sources in the same way as do isotopic ratios (Hofmann and Jochum, 1996), with the advantage that there is no need to apply in situ radioactive corrections.

Based on Nd–Sr–Pb isotope systematics, the Guyana magmas were clearly derived from a depleted mantle source (Fig. 9). They generally lie on a mixing line between N-MORB and EMII component (Fig. 8a–d), close to the so-called prevalent mantle (PREMA of Zindler and Hart, 1986). Similar conclusions arise from VICE/VICE ratios such as Th/La vs. Th/Ba, which are quasi constant in Guyana tholeiites, clustering in the PREMA field (after Hofmann and Jochum, 1996) between MORB and EMII fields (Fig. 12). Similar source characteristics arise for the high-Ti magmas emplaced in Liberia and in Brazil, taking into account the isotope and trace element data available (Figs. 9 and 12).

In Guinea, sample GUI74, assumed to be the best approximation of the mantle source, has much less radiogenic Nd and more radiogenic Sr, compared to Guyana, and lies close to the bulk silicate Earth (BSE; Fig. 9). According to Nd–Sr–Pb isotope systematics, the Guinea mantle source requires a greater involvement of EMII component (or a mixture of EMII and EMI) at the expense of N-MORB component (Fig. 8a–d). This more enriched signature is confirmed by VICE/VICE ratio, which is shifted towards the EMII field (Fig. 12), and by the LILE/HFSE enrichment distinguishing Guinea from Guyana (Fig. 6). Other low-Ti CAMP rocks from West Africa, South America, North America and Europe, which are free from significant crustal contamination (with the highest $^{143}Nd/^{144}Nd$ and lowest $^{87}Sr/^{86}Sr$ ratios), cluster in proximity to sample GUI74 in respect of either their isotopic (Fig. 9) or their VICE/VICE (Fig. 12) ratios. In the Nd–Sr isotope plot, they define a limited range, from which the fan-shaped low-Ti array diverges, which might represent the source of the low-Ti CAMP magmas.

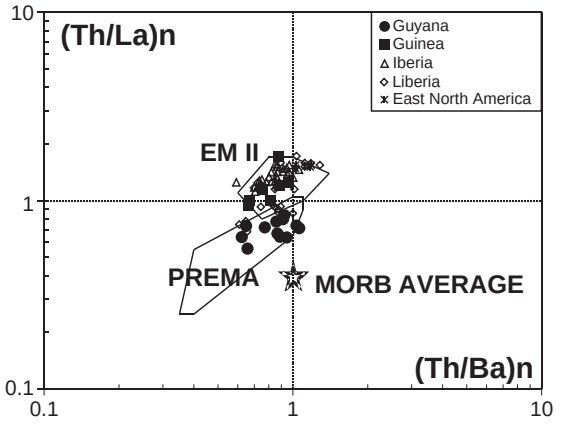

Fig. 12. Comparison of the Guyana and Guinea samples, Messejana (Cebriá et al., 2003), Liberia (Dupuy et al., 1988) and East North America (Dostal and Dupuy, 1984; Heatherington and Mueller, 1991) with reference mantle sources (Hofmann and Jochum, 1996) in the Th/La vs. Th/Ba, both ratios being normalized to primitive mantle.

To explain the EMII-type enrichment observed in Guinea, we favour a source that may have experienced mantle metasomatism through fluid release during ancient subduction processes. This source was prevalent at the origin of the low-Ti magmas throughout the CAMP, and plausibly represents a heterogeneous part of the continental lithospheric thermal boundary layer. This lithospheric source may have interacted with the N-MORB depleted source, as suggested by the EMII-N-MORB mixing relationships observed in Nd–Sr–Pb isotope plots (Fig. 8a–d). The depleted PREMA-like signature of Guyana magmas requires a greater contribution of the N-MORB asthenospheric source, as PREMA is probably not a physically distinct reservoir but the product of an efficient and widespread mixing process between mantle reservoirs. It has to be noted that neither Guinea nor Guyana magmas display radiogenic ^{206}Pb ($(^{206}Pb/^{204}Pb)_i$ from 17.95 to 18.47; Table 2, Fig. 8b–d). These low ratios are in the same range as the few Pb-isotope data available on other CAMP material (Pegram, 1990; Jourdan et al., 2003) and do not bear the HIMU signature diagnostic of the mantle plumes (Cape Verde, Fernando do Noronha, Asuncion), which might have been in a favourable position in late Triassic time to initiate the central Atlantic rifting (Morgan, 1983). The active role of a mantle plume head as initiating CAMP (White and McKenzie, 1989; Hill, 1991; Wilson, 1997; Oyarzun et al., 1997; Ernst and Buchan, 2002) is therefore questioned, as recently discussed on the basis of

geological and geochemical arguments (McHone, 2000; Puffer, 2001).

CAMP occurrences are often (although not exclusively) located on the craton edges or on adjacent mobile belts, either Pan-African, Caledonian or Hercynian (Fig. 1; Vauchez et al., 1997; Tommasi and Vauchez, 2001; DeMin et al., 2003). Along these suture zones, the lithosphere presents an asymmetrical thickness (thicker below the craton than below the mobile belt, Black and Liégeois, 1993; Anderson, 1994) and a mechanical anisotropy (Tommasi and Vauchez, 2001), which may trigger edge-driven convection, CFB production and continental rifting. Applied to CAMP genesis, this scenario, fundamentally based on pre-existing lithospheric heterogeneities, represents a viable alternative (Anderson, 1994) or complement (Courtillot et al., 1999) to the active plume head models. Assuming, as generally accepted, that melting producing the prominent low-Ti magmas dominantly occurs in the lithosphere, the heat supply required may result from a thermal incubation under the thick continental lithosphere of the Pangaea supercontinent (shield effect), without calling for a deep mantle plume head. This alternative may account for lower magma production rate per surface unit but larger surface area (7×10^6 km^2) for CAMP than for plume-related CFBs.

The location of high-Ti tholeiites along a narrow zone in Guyana, Liberia, Cassipore (Brazil) plausibly reflects a line of preferential upwelling of the depleted asthenospheric mantle in the course of Central Atlantic Ocean rifting. As suggested by some Guyana ages younger than the CAMP peak age (Deckart et al., 1997; Nomade et al., 2002b), this high-Ti event might therefore represent, at least partly, a late stage of CAMP, isotopically transitional towards the forthcoming oceanic crust.

7. Conclusions

(1) The Central Atlantic Magmatic Province (CAMP) is associated with the early stage of Central Atlantic rifting at ca. 200 Ma. Intrusives from French Guyana/Surinam and Guinea underline the overall petrogenetic complexity of this short but areally extensive magmatic event. In Guyana, CAMP is recognized in a limited volume as slightly differentiated dykes and sills (gabbros and dolerites). In Guinea, CAMP is voluminous and composed of gabbros, dolerites, dunites and wherlites that represent tholeiites, and mafic–ultramafic cumulates replenishing thick sills and laccolith (Fouta Djalon and Kakoulima regions) and minor dykes.

(2) Guyana high-Ti tholeiites display depleted isotope signatures supporting a PREMA-like mantle source (εNd_i=+5.8, $(^{87}Sr/^{86}Sr)_i$=0.7032), plausibly representing mixing between a MORB-type mantle and EMII reservoir. Besides the isotopic signature, ratios of very incompatible elements (VICE/VICE) support this PREMA signature. Trace element modeling indicates that Guyana CAMP was generated by ca. 15% partial melting and subsequently affected by a slight fractional crystallization (5–10%) or possible AFC-process (r=0.1, Proterozoic contaminant).

(3) Guinea low-Ti suites are characterized by negative Nb–Ta anomaly, LILE enrichment and isotope signatures ranging from bulk earth to enriched compositions. Isotopes and VICE/VICE ratios indicate higher involvement of the EMII component in their mantle source. Isotope modeling for Guinea CAMP shows that the magmas have been affected by AFC-process involving a Birimian contaminant (r=0.3), and for the most differentiated compositions, by additional upper crust contamination.

(4) Magma generation for CAMP has been controlled by regional and local geodynamic conditions. CAMP is mainly located on cratonic edges or adjacent mobile belts where lithospheric discontinuities may trigger edge-driven convection, magma formation and continental rifting. Whereas widespread low-Ti magmas are supposed to originate from the lithosphere, the emplacement of less abundant isotopically depleted high-Ti magmas reflects a preferential asthenospheric upwelling that might have partly occurred during a late stage in the rifting.

Acknowledgements

The authors would like to thank Dieter Garbe-Schönberg for providing the ICP-MS facilities at the

GPI of the University of Kiel. Paul Capiez is acknowledged for XRF analyses. The paper has benefited from helpful discussion with Diego Morata. William Stone and John Bennett are friendly thanked for having checked the English of this paper. We also thank two anonymous reviewers for constructive comments.

References

Abouchami, W., Boher, M., Michard, A., Albarède, F., 1990. A major 2.1 Ga event of mafic magmatism in West Africa: an early stage of crustal accretion. J. Geophys. Res. 95B, 17605–17629.

Albarède, F., 1992. How deep do common basaltic magmas form and differentiate? J. Geophys. Res. 97B, 10997–11009.

Alibert, C., 1985. A Sr–Nd isotope and REE study of late Triassic dolerites from the Pyrenées (France) and the Messejana dyke (Spain and Portugal). Earth Planet. Sci. Lett. 73, 81–90.

Anderson, D.L., 1994. The sublithospheric mantle as the source of subcontinental flood basalts; the case against the continental lithosphere and plume head reservoir. Earth Planet. Sci. Lett. 123, 269–280.

Azambre, B., Rossy, M., Lago, M., 1987. Caractéristiques pétrologiques des dolerites tholéiitiques d'âge triasique (ophites) du domaine pyrénéen. Bull. Minéral. 110, 379–396.

Barrère, J., 1959. La presqu'île du Kaloum et le Massif du Kakoulima. Notes Serv. Géol. Prospect. Min. Afr. Occid. Fr., Dakar 2, 1–44.

Bertrand, H., 1991. The Mesozoic Tholeiitic Province of Northwest Africa: a volcano-tectonic record of the early opening of Central Atlantic. In: Kampunzu, A.B., Lubala, R.T. (Eds.), Magmatism in Extensional Structural Settings. The Phanerozoic African Plate. Springer-Verlag, Berlin, pp. 147–188.

Bertrand, H., Villeneuve, M., 1989. Témoins de l'ouverture de l'atlantique central au début du jurassique: les dolérites tholéiitiques continentales de Guinée (Afrique de l'Ouest). C. R. Acad. Sci., Paris 308 (série II), 93–98.

Bertrand, H., Dostal, J., Dupuy, C., 1982. Geochemistry of early Mesozoic tholeiites from Morocco. Earth Planet. Sci. Lett. 58, 225–239.

Bertrand, H., Liegeois, J.P., Deckart, K., Féraud, G., 1999. High-Ti tholeiites in Guyana and their connection with the Central Atlantic CFB province: elemental and Nd-Sr-Pb isotopic evidence for preferential zone of mantle upwelling in course of rifting. AGU spring meeting (Abst. p.317).

Black, R., Liégeois, J.P., 1993. Cratons, mobile belts, alkaline rocks and continental lithospheric mantle: the Pan-African testimony. J. Geol. Soc. (Lond.) 150, 89–98.

Boher, M., Abouchami, W., Michard, A., Albarède, F., Arndt, N.T., 1992. Crustal growth in West Africa at 2.1 Ga. J. Geophys. Res. 97, 345–369.

Bosma, W., Kroonenberg, S.B., Van Lissa, R.V., Maas, K., de Roever, E.W.F., 1983. Igneous and metamorphic complexes of the Guiana Shield in Suriname. Geol. Mijnb. 62, 241–254.

Bryan, W.B., Frey, F.A., Thompson, G., 1977. Oldest Atlantic sea-floor: Mesozoic basalts from western North Atlantic margin and eastern North America. Contrib. Mineral. Petrol. 64, 223–242.

Bullard, E., Everett, J.E., Smith, A.G., 1965. The fit of the continents around the Atlantic. In: Bickett, P.M.S., Bullard, E., Runcorn, S.K. (Eds.), A Symposium on Continental Drift, Philos. Trans. R. Soc. Lond., A, vol. 258, pp. 41–51.

Caen-Vachette, M., 1988. Le craton ouest-africain et le bouclier guyanais: un seul craton au Protérozoïque inférieur? J. Afr. Earth Sci. 7, 479–488.

Cebriá, J.M., López-Ruiz, J., Doblas, M., Martins, L.T., Munha, J., 2003. Geochemistry of the Early Jurassic Messejana-Plasencia dyke (Portugal–Spain); implications on the origin of the Central Atlantic Magmatic Province. J. Petrol. 44, 547–568.

Choubert, B., (directeur). Carte géologique détaillée de la France, Département de la Guyane, Carte géologique à l'échelle du 1/100.000, several sheets published in different years, 1960/62/64.

Choudhuri, A., 1978a. Geochemical trends in tholeiite dykes of different ages from Guiana. Chem. Geol. 22, 79–85.

Choudhuri, A., 1978b. A microprobe study of pyroxenes from tholeiitic dykes of the Guiana Shield, South America. Neues Jahrb. Mineral., Monatsh. H6, 241–248.

Choudhuri, A., Oliveira, E.P., Sial, A.N., 1991. Mesozoic dyke swarms in northern Guiana and northern Brazil and the Cape Verde-Fernando de Noronha Vortices: a synthesis. Int. symp. of Mafic Dykes, Sao Paulo, Brazil, pp. 17–22.

Courtillot, V., Jaupart, C., Manighetti, I., Tapponnier, P., Besse, J., 1999. On causal links between flood basalts and continental breakup. Earth Planet. Sci. Lett. 166, 177–195.

Dalrymple, G.B., Gromme, C.S., White, R.W., 1975. Potassium-argon age and paleomagnetism of diabase dikes in Liberia: initiation of Central Atlantic rifting? Geol. Soc. Am. Bull. 86, 399–411.

Deckart, K., 1996. Etude du magmatisme associé au rifting de l'Atlantique Central et Sud: géochronologie 40Ar/39Ar et geóchimie sur les intrusions jurassiques de Guinée et Guyane française/Surinam, et crétacées du Brésil. Unpublished Thèse d' Université, Géoscience Azur, Documents et travaux no. 2, Université de Nice-Sophia Antipolis.

Deckart, K., Féraud, G., Bertrand, H., 1997. Age of Jurassic continental tholeiites of French Guyana, Surinam and Guinea: implications for the initial opening of the Central Atlantic Ocean. Earth Planet. Sci. Lett. 150, 205–220.

DeMin, A., Piccirillo, E.M., Marzoli, A., Bellieni, G., Renne, P.R., Ernesto, M., Marques, L., 2003. The Central Atlantic Magmatic Province (CAMP) in Brazil: petrology, geochemistry, $^{40}Ar/^{39}Ar$ ages, paleomagnetism and geodynamic implications. The central Atlantic magmatic province: insights from fragments of Pangea, AGU Geophys. Monogr., vol. 136, pp. 209–226.

De Paolo, D.J., 1981. Trace element and isotopic effects of combined wallrock assimilation and fractional crystallization. Earth Planet. Sci. Lett. 53, 189–202.

Diallo, D., Galperov, G., 1984. Tectonique de la Guinée occidentale. Pangea 2, 20–27.

Diallo, D., Bertrand, H., Azambre, B., Gregoire, M., Caseiro, J., 1992. Le complexe basique-ultrabasique du Kakoulima (Guinée-Conakry): une intrusion tholeiitique stratifiée liée au

rifting de l'Atlantique central. C. R. Acad. Sci., Paris 314 (série II), 937–943.

Dostal, J., Dupuy, C., 1984. Geochemistry of the North Mountain Basalts (Nova Scotia, Canada). Chem. Geol. 45, 245–261.

Dunning, G.R., Hodych, J.P., 1990. U/Pb zircon and baddeleyite ages for the Palisades and Gettysburg sills of the northeastern United States: implications for the age of the Triassic/Jurassic boundary. Geology 18, 795–798.

Dupuy, C., Dostal, J., 1984. Trace element geochemistry of continental tholeiites. Earth Planet. Sci. Lett. 67, 61–69.

Dupuy, C., Marsh, J., Dostal, J., Michard, A., Testa, S., 1988. Asthenospheric and lithospheric sources for Mesozoic dolerites from Liberia (Africa): trace element and isotopic evidence. Earth Planet. Sci. Lett. 87, 100–110.

Ernst, R.E., Buchan, K.L., 2002. Maximum size and distribution in time and space of mantle plumes: evidence from large igneous provinces. J. Geodyn. 31, 309–342.

Garbe-Schönberg, C.-D., 1993. Simultaneous determination of 37 trace elements in 28 international rock standards by ICP-MS. Geostand. Newsl. 17, 81–97.

Gibbs, A.K., Barron, C.N., 1983. The Guiana Shield reviewed. Episodes 6, 7–14.

Govindaraju, K., 1989. Compilation of working values and sample description for 272 geostandards. Geostand. Newsl. 13, 113 (Spec. Issue).

Gruau, G., Martin, H., Leveque, B., Capdevila, R., 1985. Rb–Sr and Sm–Nd geochronology of lower Proterozoic granite-greenstone terrains in French Guiana, South America. Precambrian Res. 30, 63–80.

Hames, W.E., Renne, P.R., Ruppel, C., 2000. New evidence for geologically instantaneous emplacement of earliest Jurassic Central Atlantic Magmatic Province basalts on the North American margin. Geology 28, 859–862.

Hawkes, D.D., 1966. The petrology of the Guiana Dolerites. Geol. Mag. 103, 320–335.

Heatherington, A.L., Mueller, P.A., 1991. Geochemical evidence for Triassic rifting in southwestern Florida. Tectonophysics 188, 291–302.

Heatherington, A.L., Mueller, P.A., 1999. Lithospheric sources of North Florida, USA tholeiites and implications for the origin of the Suwannee terrain. Lithos 46, 215–233.

Hebeda, E.H., Boelrijk, N.A.I.M., Priem, H.N.A., Verdurmen, E.A.T., Verschure, R.H., 1973. Excess radiogenic argon in the Precambrian Avanavero Dolerite in western Surinam (South America). Earth Planet. Sci. Lett. 20, 189–200.

Hill, R.I., 1991. Starting plumes and continental break-up. Earth Planet. Sci. Lett. 104, 398–416.

Hofmann, A.W., 1988. Chemical differentiation of the Earth, the relationship between mantle, continental crust, and oceanic crust. Earth Planet. Sci. Lett. 90, 297–314.

Hofmann, A.W., Jochum, K.P., 1996. Source characteristics derived from very incompatible trace elements in Mauna Loa and Mauna Kea basalts, Hawaii scientific drilling project. J. Geophys. Res. 101 (B5), 11.831–11.839.

Hurley, P.M., Leo, G.W., White, R.H., Fairbairn, H.W., 1971. Liberian age province (about 2700 m.y.) and adjacent provinces in Liberia and Sierra Leone. Geol. Soc. Amer. Bull. 82, 3483–3490.

Ionov, D.A., Savoyant, L., Dupuy, C., 1992. Application of the ICP-MS technique to trace element analysis of peridotites and their minerals. Geostand. Newsl. 16, 311–315.

Janney, P.E., Castillo, P.R., 2001. Geochemistry of the oldest Atlantic crust suggests mantle plume involvement in the early history of the Central Atlantic Ocean. Earth Planet. Sci. Lett. 192, 291–302.

Jourdan, F., Marzoli, A., Bertrand, H., Cosca, M., Fontignie, D., 2003. The northernmost CAMP: $^{40}Ar/^{39}Ar$ age, petrology and Sr–Nd–Pb isotope geochemistry of the Kerforne dyke, Brittany, France. In: Hames, W.E., McHone, J.G., Renne, P.R., Ruppel, C. (Eds.), The Central Atlantic Magmatic Province: Insights from Fragments of Pangea, AGU Geophys. Monogr., vol. 136, pp. 209–226.

Klein, E.M., Langmuir, C.H., 1987. Global correlations of ocean ridge basalt chemistry with axial depth and crustal thickness. J. Geophys. Res. 92, 8089–8115.

Lacroix, A., 1905. Les roches éruptives basiques de la Guinée française. C. R. Acad. Sci., Paris 140, 410–413.

Ledru, P., Pons, J., Miles, J.P., Feybesse, J.L., Johan, V., 1991. Transcurrent tectonics and polycyclic evolution in the lower Proterozoic of Senegal-Mali. Precambrian Res. 50, 337–354.

Liégeois, J.P., Claessens, W., Camara, D., Klerkx, J., 1991. Short-lived Eburian orogeny in southern Mali. Geology, tectonics, U–Pb and Rb–Sr geochronology. Precambrian Res. 50, 111–136.

Liégeois, J.P., Black, R., Navez, J., Latouche, L., 1994. Early and late Pan-African orogenies on the Aïr assembly of terranes (Tuareg shield, Niger). Precambrian Res. 67, 59–88.

Marzoli, A., Renne, P.R., Piccirillo, E.M., Ernesto, M., DeMin, A., 1999. Extensive 200-millon-year-old continental flood basalts of the Central Atlantic Magmatic Province. Science 284, 616–618.

Mauche, R., Faure, G., Jones, L.M., Hoefs, J., 1989. Anomalous isotopic compositions of Sr, Ar, and O in the Mesozoic diabase dikes of Liberia, West Africa. Contrib. Mineral. Petrol. 101, 12–18.

May, P.R., 1971. Patterns of Triassic diabase dikes around the North Atlantic in the context of predrift position of the continents. Geol. Soc. Amer. Bull. 82, 1285–1292.

McHone, G.J., 2000. Non-plume magmatism and rifting during the opening of the Central Atlantic Ocean. Tectonophysics 316, 287–296.

Morgan, W.J., 1983. Hotspot tracks and the early rifting of the Atlantic. Tectonophysics 94, 123–139.

Nomade, S., Pouclet, A., Chen, Y., 2002a. The French Guyana doleritic dykes: geochemical evidence of three populations and new data for the Jurassic Central Atlantic Magmatic Province. J. Geodyn. 34, 595–614.

Nomade, S., Féraud, G., Renne, P., Chen, Y., 2002b. New $^{40}Ar/^{39}Ar$ ages for Central Atlantic Magmatic Province in French Guyana: a younger volcanism? Geochim. Cosmochim. Acta 66 (S1), A559.

Oliveira, E.P., Tarney, J., Joao, X.J., 1990. Geochemistry of the Mesozoic Amapá and Jari Dyke Swarms, N-Brazil: plume related magmatism during the opening of the Central Atlantic. In: Parker, A.J., Rickwood, P.C., Tucker, D.H. (Eds.), Mafic

Dykes and Emplacement Mechanism. Balkema, Rotterdam, pp. 173–183.

Oyarzun, R., Doblas, M., López-Ruiz, J., Cebriá, J.M., 1997. Opening of the Central Atlantic and asymmetric mantle upwelling phenomena: implications for long-lived magmatism in western North Africa and Europe. Geology 25, 727–730.

Pegram, W.J., 1990. Development of continental lithospheric mantle as reflected in the chemistry of the Mesozoic Appalachian Tholeiites, U.S.A.. Earth Planet. Sci. Lett. 97, 316–331.

Poitrasson, F., Pin, C.H., Telonk, P., Imbert, J.-L., 1993. Assessment of a simple method for the determination of Nb and Ta at the sub-μg/g (ppm) level in silicate rocks by ICP-MS. Geostand. Newsl. 17, 209–215.

Priem, H.N.A., Boelrijk, N.A.I.M., Hebeda, E.H., Verdurmen, E.A.Th., Verschure, R.H., 1968. Isotopic age determinations on Surinam rocks: 4. Ages of basement rocks in north-western Surinam and of the Roraima tuff at Tafelberg. Geol. Mijnb. 47, 191–196.

Priem, H.N.A., Boelrijk, N.A.I.M., Hebeda, E.H., Verdurmen, E.A.TH., Verschure, R.H., 1971. Isotopic ages of the Trans-Amazonian acidic magmatism and the Nickerie Metamorphic episode in the Precambrian basement of Suriname, South America. Geol. Soc. Amer. Bull. 82, 1667–1680.

Priem, H.N.A., Boelrijk, N.A.I.M., Hebeda, E.H., Verdurmen, E.A.T.H., Verschure, R.H., 1973. Age of the Precambrian Roraima formation in northeastern South America: evidence from isotopic dating of Roraima pyroclastic volcanic rocks in Suriname. Geol. Soc. Amer. Bull. 84, 1677–1684.

Priem, H.N.A., Boelrijk, N.A.I.M., Hebeda, E.H., Kroonenberg, S.B., Verdurmen, E.A.Th., Verschure, R.H., 1977. Isotopic ages in the high-grade metamorphic Coeroeni group, southwestern Suriname. Geol. Mijnb. 56, 155–160.

Puffer, J.H., 2001. Contrasting high field strength element contents of continental flood basalts from plume versus reactivated-arc-sources. Geology 29, 675–678.

Rapaille, C., Marzoli, A., Bertrand, H., Féraud, G., Reisberg, L., Fontignié, D., 2003. Geochemistry and $^{40}Ar/^{39}Ar$ age of the European part of the Central Atlantic Magmatic Province. EUG-AGU-EGS Joint Assembly, Nice.

Roelands, I., 1990. Inductively coupled plasma determination of nine rare-earth elements in sixty international geochemical reference samples. Geostand. Newsl. 14, 137–147.

Sebai, A., Féraud, G., Bertrand, H., Hanes, J., 1991. $^{40}Ar/^{39}Ar$ dating and geochemistry of tholeiitic magmatism related to the early opening of the Central Atlantic rift. Earth Planet. Sci. Lett. 104, 455–472.

Steiger, R.H., Jäger, E., 1977. Subcommission on geochronology: convention of the use of decay constants in geo- and cosmochronology. Earth Planet. Sci. Lett. 36, 359–362.

Sun, S.S., McDonough, W.F., 1989. Chemical and isotopic systematics of oceanic basalts: implications for mantle composition and processes. In: Saunders, A.D., Norry, M.J. (Eds.), Magmatism in the ocean basins, Geol. Soc. Spec. Publ., vol. 42, pp. 313–345.

Taylor, S.R., McLennan, S.M., 1985. The continental crust: its composition and evolution. Blackwell Scientific Publications. 312 p.

Tommasi, A., Vauchez, A., 2001. Continental rifting parallel to ancient collisional belts: an effect of the mechanical anisotropy of the lithospheric mantle. Earth Planet. Sci. Lett. 185, 199–210.

Vauchez, A., Barruol, G., Tommasi, A., 1997. Why do continents break-up parallel to ancient orogenic belts? Terra Nova 9, 62–66.

Villeneuve, M., Cornée, J.-J., 1994. Structure, evolution and palaeogeography of the West African Craton and bordering belts during the Neoproterozoic. Precambrian Res. 69, 307–326.

Weigand, P.W., Ragland, P.C., 1970. Geochemistry of Mesozoic dolerite dikes from eastern north America. Contrib. Mineral. Petrol. 29, 195–214.

White, R., McKenzie, D., 1989. Magmatism at rift zones: the generation of volcanic continental margins and flood basalts. J. Geophys. Res. 94, 7685–7729.

Wilson, M., 1997. Thermal evolution of the Central Atlantic passive margins: continental break-up above a Mesozoic super-plume. J. Geol. Soc. (Lond.) 154, 491–495.

Zindler, A., Hart, S.R., 1986. Chemical geodynamics. Annu. Rev. Earth Planet. Sci. 14, 493–571.